V. HYDRODYNAMIC MODELING

V.1 INTRODUCTION

This section summarizes field data collection effort and the development of a hydrodynamic model for the Nantucket Harbor estuary system, on the island of Nantucket. For this system, the final calibrated model offers an understanding of water movement through the estuary, and provides the first step towards evaluating water quality, as well as a tool for later determining nitrogen loading "thresholds". Nutrient loading data combined with measured environmental parameters within the system become the basis for an advanced water quality model based on total nitrogen concentrations. This type of model provides a tool for evaluating existing estuarine water quality parameters, as well as determining the likely positive impacts of various alternatives for improving overall estuarine health, facilitating the understanding how pollutant loadings into the estuary will affect the biochemical environment and its ability to sustain a healthy marine habitat.

In general, water quality studies of tidally influenced estuaries must include a thorough evaluation of the hydrodynamics of the estuarine system. Estuarine hydrodynamics control a variety of coastal processes including tidal flushing, pollutant dispersion, tidal currents, sedimentation, erosion, and water levels. Numerical models provide a cost-effective method for evaluating tidal hydrodynamics since they require limited data collection and may be utilized to numerically assess a range of management alternatives. Once the hydrodynamics of an estuary system are understood, computations regarding the related coastal processes become relatively straightforward extensions to the hydrodynamic modeling. For example, the spread of pollutants may be analyzed from tidal current information developed by the numerical models.

Coastal embayments like the Nantucket Harbor system are the initial recipients of freshwater flows (i.e., groundwater and surfacewater) and the nutrients they carry. An embayment's shape influences the time that nutrients are retained in them before being flushed out to adjacent open waters, and their shallow depths both decrease their ability to dilute nutrient (and pollutant) inputs and increase the secondary impacts of nutrients recycled from the sediments. Degradation of coastal waters and development are tied together through inputs of pollutants in runoff and groundwater flows, and to some extent through direct disturbance, i.e. boating, oil and chemical spills, and direct discharges from land and boats. Excess nutrients, especially nitrogen, promote phytoplankton blooms and the growth of epiphytes on eelgrass and attached algae, with adverse consequences including low oxygen, shading of submerged aquatic vegetation, and aesthetic problems.

A hydrodynamic study was performed for the Nantucket Harbor system, which is located on the island of Nantucket, south of Cape Cod. A section of a topographic map in Figure V-1 shows the general study area. The Nantucket Harbor system has many attached sub-systems, with the three main sub-divisions: 1) the main harbor basin,2) the Head of the Harbor and 3) Polpis Harbor. The entire Nantucket Harbor system has a surface coverage of 4,830 acres, including the attached sub-embayments. Polpis Harbor is the largest sub-embayment of the Harbor system, with a 280 acre coverage, including Pocomo Meadow.

Circulation in the Nantucket Harbor system is dominated by tidal exchange with Nantucket Sound. The Harbor is connected to Nantucket Sound through a broad, structured inlet. The inlet jetties are each over 3,500 ft long and are highly permeable due to their low elevation and general condition. An 80-foot-wide cut near the base of the east jetty allows the passages of boating traffic. There is little attenuation of the tide range between the inlet and Head of the

Harbor. This indicates that there is little loss of tidal energy through the system, either due to bottom friction in shallow areas or from channel restrictions, e.g., between some of the cuspate formations that are a distinguishing hallmark of the Harbor shoreline.

Figure V-1. Topographic map detail of Nantucket Harbor, Nantucket Island, Massachusetts.

This hydrodynamic study proceeded as two component efforts. In the first portion of the study, bathymetry, tide, and circulation velocity data were collected in order to accurately characterize the physical system, and to provide data necessary for the modeling portion of the study. The bathymetry survey of Nantucket Harbor was performed to determine the present variation of embayment and channel depths throughout the system. The recent bathymetry survey data were supplemented using historical NOAA data (NOAA, 2001) in the offshore region near the inlet. In addition to bathymetry, tides were recorded at seven locations within the Harbor system for 31 days. These tide data were necessary to run and calibrate the hydrodynamic model of the system. Finally, an Acoustic Doppler Current Profiler (ADCP) survey was completed during a single tide cycle to measure ebb and flood velocities across two channel transects. The ADCP data were used to compute system flow rates and to provide an independent means of verifying the performance of the hydrodynamic model.

A numerical hydrodynamic model of the Nantucket Harbor system was developed in the second portion of this analysis. Using the bathymetry survey data, a model grid mesh was generated for use with the RMA-2 hydrodynamic code. The tide data from offshore in Nantucket Sound were used to define the open boundary conditions that drive the circulation of

the model at the system inlet, and data from the five TDR stations within the system were used to calibrate and verify model performance to ensure that it accurately represents the dynamics of the real, physical system.

The calibrated computer model of the Harbor was used to compute the flushing rates of selected sub-sections. Though water quality in an embayment cannot be directly inferred by use of computed flushing rates alone, they can serve as useful indicators of embayment flushing performance relative to other areas in the same system. The ultimate utility of this hydrodynamic model is as input into a constituent transport model, where water quality constituents like nitrogen are modeled to determine the real water quality dynamics of a system.

V.2 GEOMORPHIC AND ANTHROPOGENIC EFFECTS TO THE ESTUARINE SYSTEM

From a coastal processes perspective, the northern shoreline of Nantucket is a relatively quiescent region. Although natural wave and tidal forces continue to reshape the shoreline, day-to-day conditions have limited impact on the shoreline migration and/or inlet stability. In addition, the net direction of longshore sediment transport varies along the north shore of Nantucket, primarily as a result of the variable shoreline orientation relative to the dominant wave direction. In general the littoral drift is from west-to-east along the shoreline to the west of Nantucket Harbor inlet and east-to-west along the shoreline to the east of the inlet. Evidence of this long-term sediment transport direction is a build-up of sand, resulting in historical shoreline accretion, to the west of the west jetty and to the east of the east jetty.

In contrast to the mild day-to-day conditions, typical northeast storms and infrequent hurricane events (e.g. the 1944 Hurricane and Hurricane Carol in 1954) can cause overwash of Coatue Beach. Northeast storm events (causing waves to approach the Nantucket shoreline from the east and northeast) create a sediment transport reversal from typical conditions west of the inlet; however, these transport reversals are typically short-lived and have little effect over inlet processes. Unlike many areas along the nearby Cape Cod shoreline, the Nantucket shoreline experiences similar storm surge levels from both major northeasters and hurricanes. Over the past 50 years, the largest storm surge observed in Nantucket Harbor occurred during a northeast storm in March 1956, where water elevations between 5.2 and 6.2 feet above Half Tide Level (HTL) were measured in the harbor.

V.2.1 Inlet Stabilization

Due to the quiescent wave environment and small tide range in the vicinity of the Nantucket Harbor inlet, as well as the large jetties protecting the channel, inlet migration and stability are not a concern for Nantucket Harbor. Figure V-2 shows the position of the inlet in 1890, prior to construction of jetties needed to stabilize the navigation channel. Before the jetties were constructed, significant shoaling within the inlet channel limited Nantucket Harbors use as a commercial port. Construction records indicate that rubble mound jetty construction at Nantucket Harbor was initiated in 1881 and completed in 1907. The east and west rubble-mound jetties were constructed to lengths of 6,987 and 4,955 ft, respectively. The jetties converged to a distance of approximately 1,000 ft, with the east jetty extending 800 ft seaward of the west jetty. Crown elevations of the jetties were typically +5 ft MLW, with side slopes of 1:1 (vertical: horizontal) and crest widths of 4 and 6 ft on the west and east jetties, respectively. Approximately 63,000 tons of stone were used to construct the east jetty and 59,000 tons of stone were used in the west jetty. Due to the relatively large scale and low construction elevation, jetty repairs and improvements have become commonplace for the structures. Major jetty repairs and/or improvements occurred in 1917, 1926, 1936, and 1962. The 1941 configuration of the inlet with jetties is shown in Figure V-3 and is similar to the existing

configuration. Settling of the jetties since construction and/or repair allows water to flow across the structures when water levels exceed mid-tide level.

Figure V-2 A portion of the U.S.G.S. 1890 map showing Nantucket Harbor. This map depicts the condition of this inlet prior to the installation of jetties.

V.2.2 Inlet Processes and Shoreline Change Analysis

Since inlet stability is partially governed by longshore coastal sediment transport, understanding the regional long-term shoreline change and littoral movement of sand is critical for evaluating stability of Nantucket Harbor inlet. As discussed above, the observed longshore transport rates are relatively low, primarily as a result of the quiescent wave environment of Nantucket Sound. Although the amount of sand moving along the coast is small, the tidal prism through the Nantucket Harbor entrance is relatively large. Since the construction of the jetty system at the entrance, the inlet has generally reached equilibrium and the significant tidal velocities through the main channels are sufficient to inhibit shoaling.

Shoreline change maps can effectively be used to evaluate the effects of long-term coastal processes. In addition, shoreline change maps also can indicate the effects of short-term changes that often occur as the result of anthropogenic (e.g. development of extensive shore protection structures) or natural (e.g. inlet migration) processes. Prior to developing conclusions and/or management recommendations that depend on shoreline change estimates, it is critical to understand potential errors and uncertainties associated with this type of analysis. Understanding the limitations of shoreline change data is critical for developing appropriate management strategies for shorelines and inlets such as the entrance to Nantucket's Harbor.

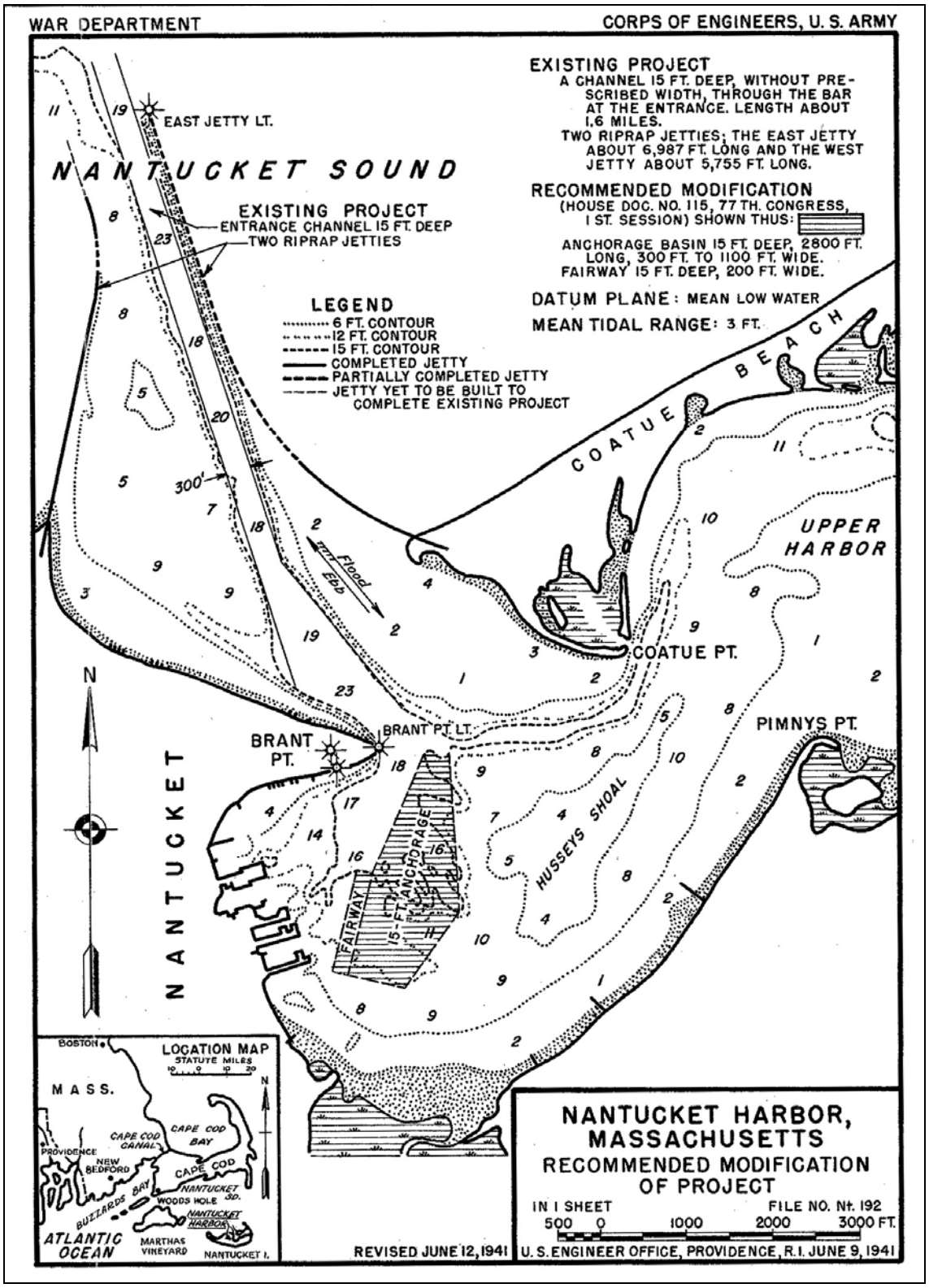

Figure V-3. Recommended navigation improvements for Nantucket Harbor, based on the 1941 U.S. Army Corps of Engineers plan.

Shoreline change was evaluated for this study during the time period from 1955 to 2003. The 1955 shoreline was digitized from the National Ocean Service (NOS) T-Sheets. The shorelines depicted on the T-sheets were created by interpreting the high-water shoreline position from controlled aerial photography. The 2003 shoreline was developed by compiling high-water shoreline position from April 2003 color orthophotographs available from MassGIS. The high-water shoreline visible on the orthophotos was digitized by hand using a line-drawing tool in ArcGIS 9.0. Although the high-water shoreline was well marked in most areas, in some instances it was difficult to discern the high-water line based on coloration and other visible features alone. For these areas, NOAA's LIDAR survey from September 25, 2000 was used to aid in the determination of shoreline position.

Change calculations were made at 40-meter (131 foot) intervals along the outer coast from Jetties Beach, extending across the Nantucket Harbor to Coatue Beach using the Automated Shoreline Analysis Program (ASAP) for ArcGIS 9.0. Shore-normal transects were developed using average shoreline angles determined at each analysis point. All transects used for determining change rates were visually inspected to ensure that each was suitability located and properly oriented.

Shoreline change calculated between 1955 and 2003 (Figure V-4) shows little change along Jetties Beach, west of the entrance to Nantucket Harbor. This area shows change rates which are generally less than ±0.7 feet per year. Directly adjacent to the west jetty, an average accretion of about 2 feet per year is seen. The beach shape had stabilized following the jetty construction around 1900 and this residual accretion is due to the sheltering from the structure itself. The area immediately inside the west jetty has accreted at a rate of nearly 5 feet per year, due primarily to sand from Jetties Beach leaking over and through the west jetty. Continuing out towards Brant Point, the central portion of the beach has seen little change in the past 48 years, while the eastern tip near Brant Point Light has seen erosion of approximately 2 feet per year.

Across the harbor entrance, the shoreline has accreted along the first 4000 feet or so adjacent to the east jetty. The shoreline change rate is +4-5 feet per year immediately next to the jetty and gradually decreases to the east along Coatue Beach. This area of accretion abuts a similarly sized section of erosion which is centered opposite Second Point on the harbor side of the beach. This 4000 foot reach of shoreline has seen erosion of 2-3 feet per year. The remainder of Coatue Beach shows perhaps a slight accretion on average, but in general this reach of shoreline has seen little change.

V.2.3 Inlet Management Implications

For the tidal inlet to Nantucket Harbor, the influence of shoreline change and the related longshore sediment transport rates directly influence the stability of the existing inlet systems. According to the shoreline change analysis, the shoreline is accreting along both sides of the inlet. In addition, accretion within the inlet throat has increased beach widths at the base of the jetties within the entrance channel. Continued settling of the structures will allow shoaling to increase; however, this increase to inlet shoaling rates will be gradual. At the present time, the inlet to Nantucket Harbor provides for safe navigation as well as efficient tidal circulation.

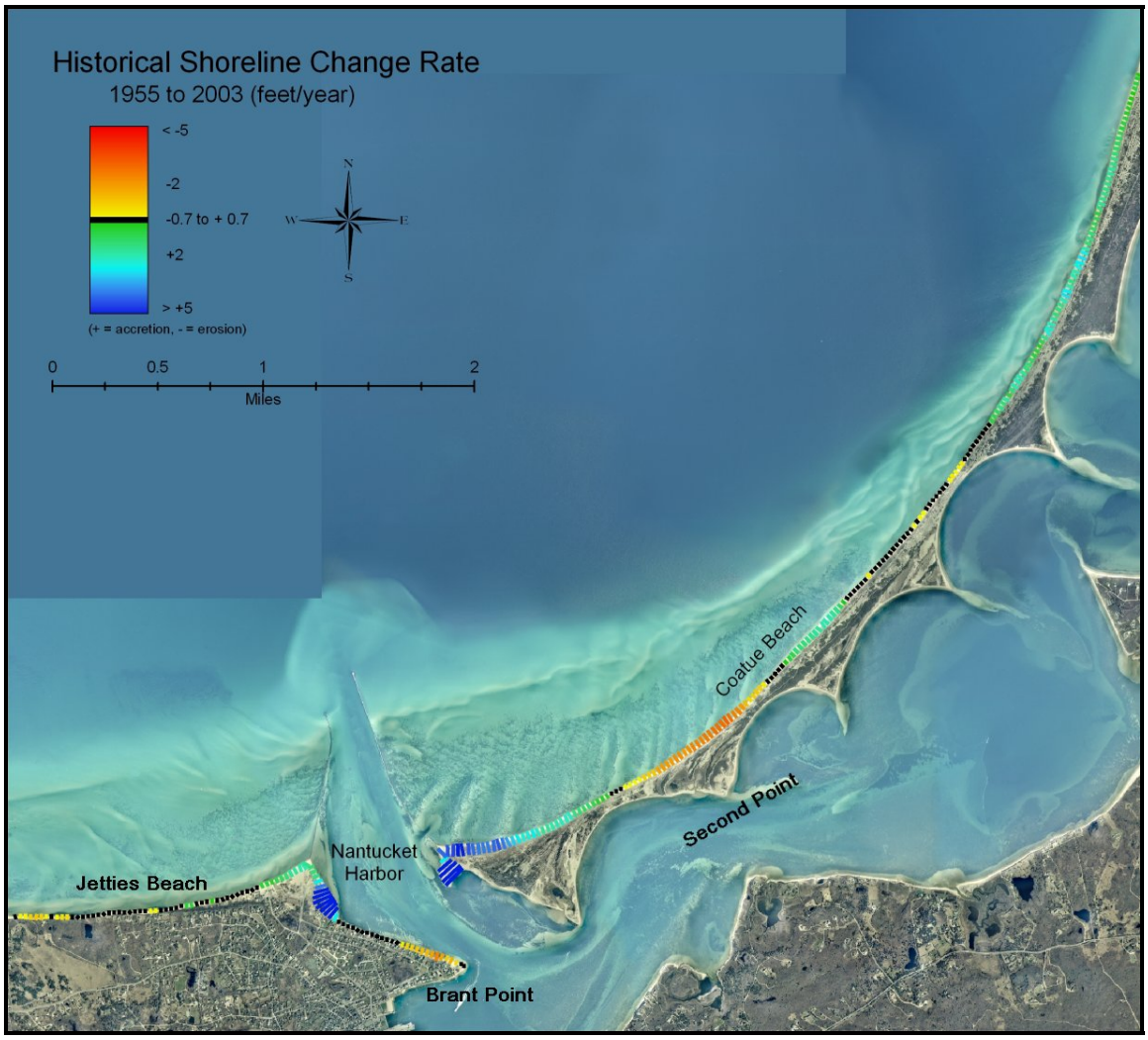

Figure V-4. Historical shoreline change rates (1955-2003) in the area of Nantucket Harbor.

V.3 DATA COLLECTION AND ANALYSIS

The field data collection portion of this study was performed to characterize the physical properties of the Nantucket Harbor estuary. Bathymetry were collected throughout the system so that it could be accurately represented in the computer hydrodynamic model and water quality model of the system. In addition to the bathymetry, tide data were also collected at six locations, to run the circulation model with real tides, and also to calibrate and verify its performance.

V.3.1 Bathymetry Data Collection

Bathymetry data in Nantucket Harbor were collected during September 2004. Supplemental offshore NOAA bathymetry were available from a 1958 survey of the Harbor vicinity. The September 2004 survey employed a bottom tracking Acoustic Doppler Current Profiler (ADCP) mounted on an inboard motor boat. Positioning data were collected using a differential GPS. The survey design included gridded transects at roughly 1000 ft spacings in along the main basin, and finer spacings at the inlet and in Polpis Harbor. Survey paths are shown in Figure V-5. The resulting bathymetric surface created by interpolating the data to a finite element mesh is shown in Figure V-6. All bathymetry was tide corrected, and referenced

to the North American Vertical Datum of 1988 (NAVD 88), using survey benchmarks located in the project area.

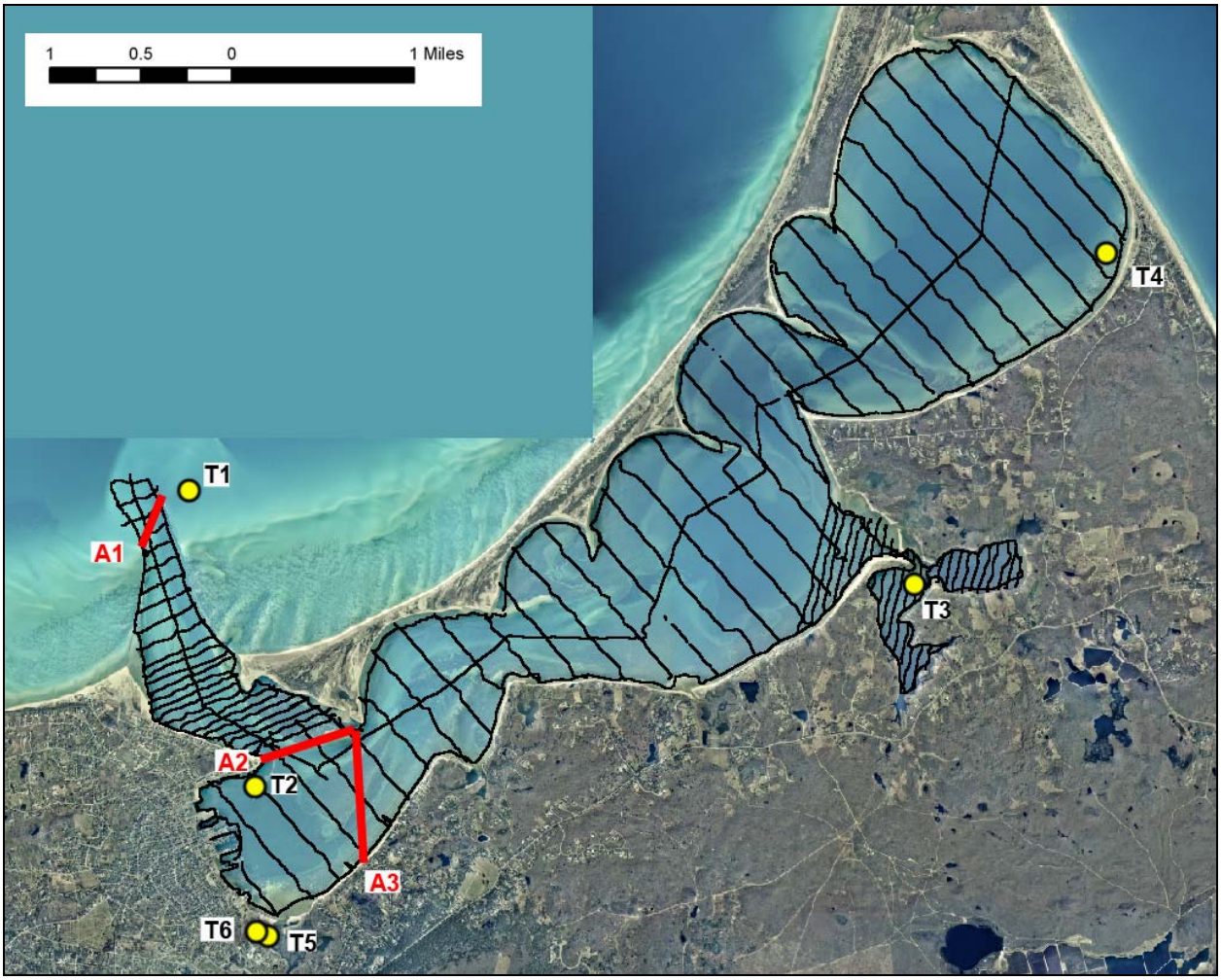

Figure V-5. Transects from the bathymetry survey of the Nantucket Harbor markers show the locations of the three tide recorders deployed for this study.

Results from the survey show that the deepest point within the Harbor is located off of Brant Point in the navigation channel, and is -33.9 ft NAVD. Other deep regions of the Harbor include the basin off of Polpis Harbor, which has a maximum depth of -28.0 feet, and the Head of the Harbor, which has a maximum depth of -25.2 feet, and an average depth of -9.8 feet. The maximum depth found in Polpis Harbor is -10.6 feet, and this basin has an average depth of -5.0 feet.

V.3.2 Tide Data Collection and Analysis

Tide data records were collected at six stations in the Nantucket Harbor estuary: 1) offshore the Harbor inlet, 2) Brant Point (at the USCG station), 3) Head of the Harbor, 4) Polpis Harbor, 5) The Creeks and 6) Consu Pond. The locations of the stations are shown in Figure V-11. The Temperature Depth Recorders (TDR) used to record the tide data were deployed for a 31-day period between August 30 and September 30, 2004. The elevation of each gauge was surveyed relative to NAVD 88. Duplicate offshore gauges were deployed to ensure data

recovery, since the offshore tide record is crucial for developing the open boundary condition of the hydrodynamic model of the Nantucket Harbor system. Data from Brant Point, Polpis Harbor and the Head of the Harbor were used to calibrate the model.

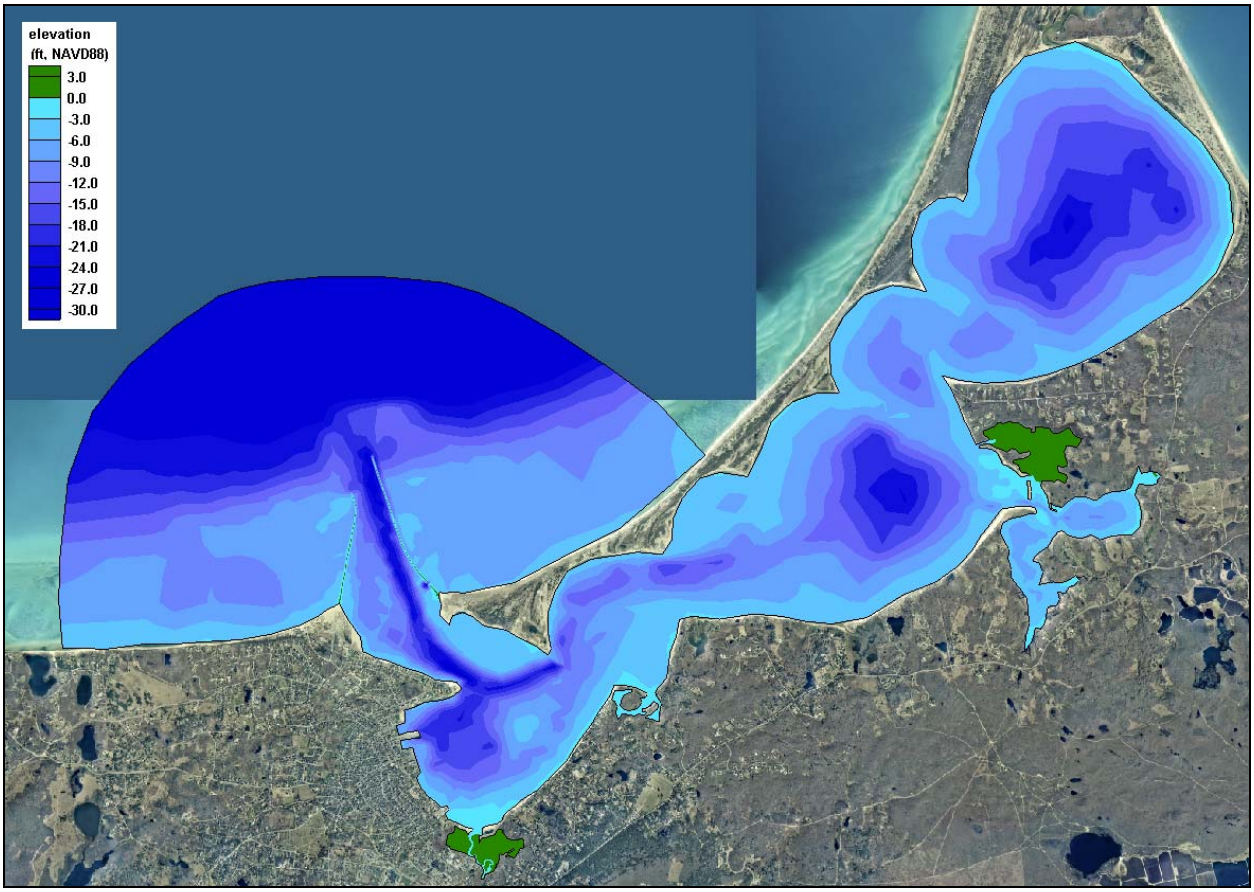

Figure V-6. Plot of interpolated finite-element grid bathymetry of the Nantucket Harbor system, shown superimposed on 2003 aerial photos of the system locale. Bathymetric contours are shown in color at three-foot intervals.

Plots of the tide data from five representative gauges are shown in Figure V-7, for the entire 31-day deployment. The spring-to-neap variation in tide can be seen in these plots. From the plot of the data from offshore Nantucket Harbor, the tide reaches its maximum spring tide range of approximately 4.0 feet around August 31, and about seven days later the neap tide range is much smaller, as small as 1.5 feet. The second spring tide should occur around September 14, the time of the new moon, but the tide range is not clearly larger than seven days earlier during the spring tide range. The causes of this odd feature of the tide in this are discussed from the results of the harmonic analysis later in this section.

A visual comparison in Figure V-8 between tide elevations at four stations in Nantucket Harbor shows that there is negligible reduction in the tide range in the upper reaches of the system. The loss of amplitude with distance from the inlet is described as tidal attenuation. Frictional mechanisms dissipate tidal flow energy, resulting in a reduction of the height of the tide. Tide attenuation is accompanied by a time delay (or phase lag) in the time of high and low tide (relative to the offshore tide), which becomes more pronounced farther into an estuary. The

tide lag greatest at the Head of the Harbor, as seen in Figure V-8, where low tide occurs approximately 90 minutes after low tide in Nantucket Sound.

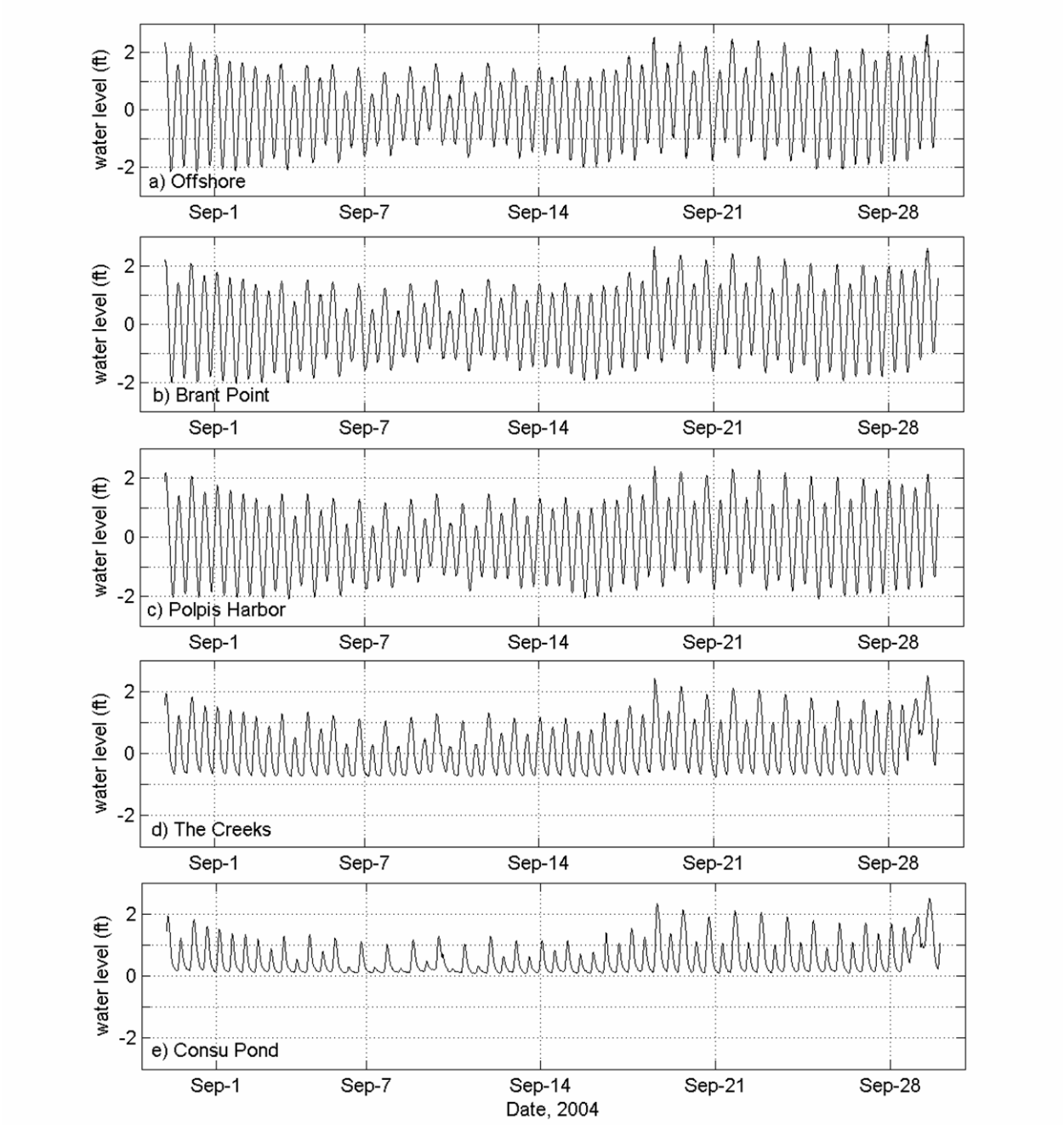

Figure V-7. Plots of observed tides for the Nantucket Harbor system, for the 31-day period between August 30 and September 30, 2004. The top plot shows tides offshore Nantucket Harbor inlet, in Nantucket Sound. Tides recorded in the Harbor at Brant Point, Polpis Harbor, The Creeks and in Consu Pond are also shown. All water levels are referenced to the **North American Vertical Datum** of 1988 (NAVD 88).

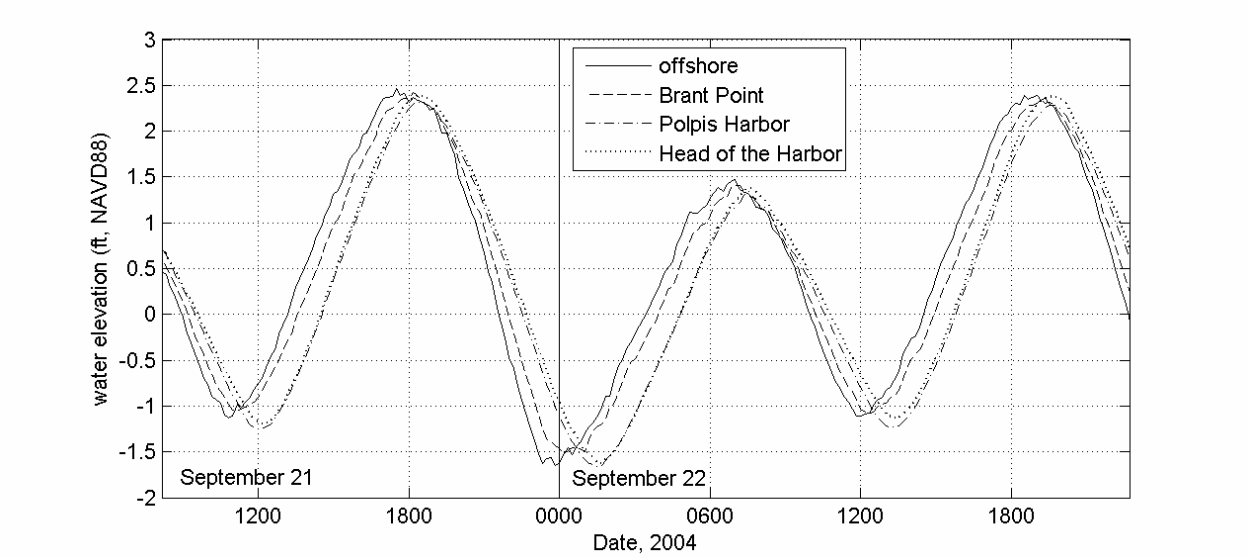

Figure V-8. Plot showing two tide cycles tides at three stations in the Nantucket Harbor system plotted together. Demonstrated in this plot is the minor frictional damping effect caused by flow restrictions at the inlets. The damping effects are seen only as a lag in time of high and low tides from Nantucket Sound. The time lag of low tide between the Sound and Prince Cove in this plot is 50 Minutes.

Standard tide datums were computed from the 31-day records. These datums are presented in Table V-1. For most NOAA tide stations, these datums are computed using 19 years of tide data, the definition of a tidal epoch. For this study, a significantly shorter time span of data was available, however, these datums still provide a useful comparison of tidal dynamics within the system. The Mean Higher High (MHH) and Mean Lower Low (MLL) levels represent the mean of the daily highest and lowest water levels. The Mean High Water (MHW) and Mean Low Water (MLW) levels represent the mean of all the high and low tides of a record, respectively. The Mean Tide Level (MTL) is simply the mean of MHW and MLW. The lack of tide attenuation through the main basin of the Nantucket Harbor estuary is apparent by how there is essentially no change in the elevation of each of the datums, from Nantucket Sound to the Head of the Harbor. A larger difference is observed in the records from The Creeks and Consu Pond, which are marsh regions. The gauge from The Creeks shows an elevated MLW and MTL, compared to the Harbor, which is typical of tides in marsh creeks. The gauge from Consu Pond shows additional increases in MLW and MTL which is due to the culvert between The Creeks and Consu Pond.

The tides in Nantucket Sound are semi-diurnal, meaning that there are typically two tide cycles in a day. There is usually a small variation in the level of the two daily tides. This variation can be seen in the differences between the MHHW and MHW, as well as the MLLW and MLW levels.

A more thorough harmonic analysis of the tidal time series was performed to produce tidal amplitude and phase of the major tidal constituents, and provide assessments of hydrodynamic 'efficiency' of the system in terms of tidal attenuation. This analysis also yielded a quantitative assessment of the relative influence of non-tidal, or residual, processes (such as wind forcing) on the hydrodynamic characteristics of the system.

A harmonic analysis was performed on the time series from each gauge location. Harmonic analysis is a mathematical procedure that fits sinusoidal functions of known frequency to the measured signal. The observed astronomical tide is therefore the sum of several individual tidal constituents, with a particular amplitude and frequency. For demonstration purposes a graphical example of how these constituents add together is shown in Figure V-9. The amplitudes and phase of 23 known tidal constituents result from this procedure. Table V-2 presents the amplitudes of eight tidal constituents in the Nantucket Harbor system.

The M_2, or the familiar twice-a-day lunar semi-diurnal tide, is the strongest contributor to the signal with an amplitude of 1.4 ft throughout the system. The total range of the M_2 tide is twice the amplitude, or 2.8 ft. The M_4 and M_6 tides are higher frequency harmonics of the M_2 lunar tide (exactly half the period of the M_2 for the M_4, and one third of the M_2 period for the M_6), results from frictional attenuation of the M_2 tide in shallow water. The M_4 has an amplitude of 0.1 feet near the system inlet, but is reduced in Polpis Harbor and the Head of the Harbor. The M_6 has a very small amplitude in the system (less than 0.1 feet at all gauge stations). There is little change in the M_2 through the main basin of the Harbor, which is a further indication that friction losses in the system are minimal, and that Nantucket Harbor flushes very efficiently, even to its farthest reaches at the Head of the Harbor.

Table V-1. Tide datums computed from a 28-day period from the tide records collected in the Nantucket Harbor system. Datum elevations are given relative to NAVD 88.

Tide Datum	Offshore	Brant Point	Polpis Harbor	Head of the Harbor	The Creeks	Consu Pond
Maximum Tide	2.6	2.7	2.4	2.4	2.4	2.3
MHHW	1.8	1.7	1.7	1.8	1.5	1.5
MHW	1.5	1.4	1.4	1.5	1.2	1.2
MTL	-0.1	-0.1	-0.2	0.0	0.3	0.7
MLW	-1.6	-1.6	-1.7	-1.6	-0.7	0.1
MLLW	-1.8	-1.7	-1.8	-1.7	-0.7	0.1
Minimum Tide	-2.2	-2.0	-2.1	-2.1	-0.8	0.1

The other major tide constituents also show little variation across the system. The diurnal tides (once daily), K_1 and O_1, possess amplitudes of approximately 0.2 feet an 0.3 feet respectively. Other semi-diurnal tides, the S_2 (12.00 hour period) and N_2 (12.66-hour period) tides, contribute significantly to the total tide signal, with amplitudes of 0.2 feet and 0.3 feet, respectively. The M_{sf} is a lunarsolar fortnightly constituent with a period of approximately 14 days, and is the result of the periodic conjunction of the sun and moon, and has an amplitude less than 0.1 ft.

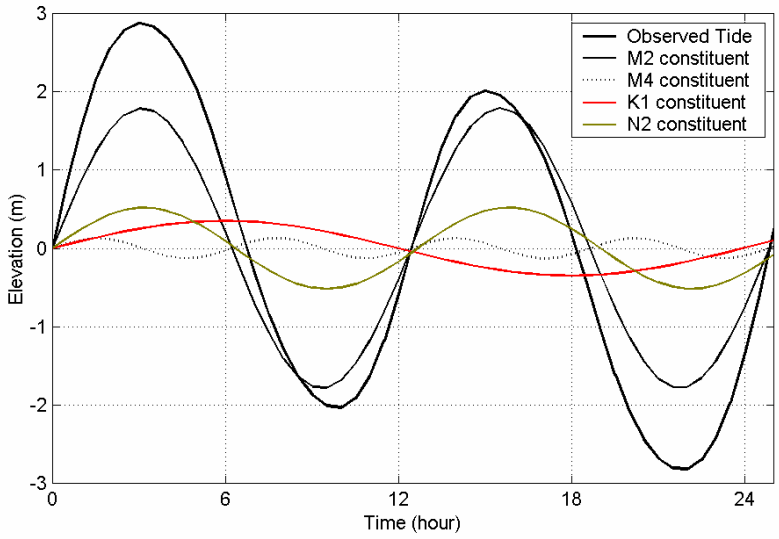

Figure V-9. Example of an observed astronomical tide as the sum of its primary constituents.

Table V-2. Major tidal constituents determined for gauge locations in Nantucket Harbor, September 30 through October 30, 2004.

	Amplitude (feet)							
Constituent	M_2	M_4	M_6	S_2	N_2	K_1	O_1	M_{sf}
Period (hours)	12.42	6.21	4.14	12.00	12.66	23.93	25.82	354.61
Nantucket Sound (offshore)	1.44	0.13	0.04	0.21	0.34	0.24	0.31	0.02
Brant Point	1.37	0.09	0.04	0.19	0.31	0.24	0.30	0.02
Polpis Harbor	1.38	0.03	0.05	0.19	0.31	0.24	0.31	0.02
Head of the Harbor	1.38	0.05	0.05	0.19	0.31	0.26	0.32	0.02
The Creeks	0.88	0.12	0.04	0.10	0.20	0.23	0.26	0.08
Consu Pond	0.45	0.15	0.04	0.07	0.17	0.18	0.20	0.07

Though there is little change in constituent amplitudes across the length of the main basin of the Harbor, the phase change of the tide is easily seen from the results of the harmonic analysis. Table V-3 shows the delay of the M_2 at different points in the Nantucket Harbor system, relative to the timing of the M_2 constituent in Nantucket Sound, offshore the Coatue shoreline. The analysis of the data from the Head of the Harbor show that there is a 71 minute delay between the inlet and the farthest reach of the system. However, the greatest delay is at the Consu Pond TDR station, a sub-embayment which is closer to the inlet, but separated by the main basin of the system by marsh and a culvert. This station also showed the largest reduction of the M_2 amplitude (Table V-2). Compared to other locations instrumented in this study, Consu Pond shows the greatest tidal attenuation.

Results of the harmonic analysis provide the reason why the transition from spring to neap tide ranges is not as apparent as it is at other areas in southeastern Massachusetts (e.g., Cape Cod Bay), as discussed earlier. The cause of the mute transition between spring and neap tide ranges is the relatively large amplitudes of the N_2 (larger lunar elliptic semidiurnal constituent) and O_1 (lunar diurnal constituent) constituents. From the analysis of other tide records from around southeastern Massachusetts, the N_2 has a typical amplitude that is less than 10% of the total tide, and the O_1 is typically less than 7% of the total tide amplitude. At Nantucket Harbor

however, the N_2 and O_1 have much larger amplitudes relative to the total tide, at 12% each. These constituents are slightly out of phase with the M_2 and K_1 (normally the greater contributors to the total tide amplitude), and therefore add and subtract from the total observed tide signal in cycles that are different (longer) than the 7 lunar day transition from spring to neap tides. In other areas (again, like Cape Cod Bay), the N_2 and O_1 represent a smaller percentage of the total observed tide, so there effect on the observed tide would be smaller.

Table V-3. M_2 tidal constituent phase delay (relative to Nantucket Sound) for gauge locations in the Nantucket Harbor system, determined from measured tide data.

Station	Delay (minutes)
Brant Point	23.6
Polpis Harbor	65.4
Head of the Harbor	70.5
The Creeks	60.2
Consu Pond	94.0

In addition to the tidal analysis, the data were further evaluated to determine the importance of tidal versus non-tidal processes to changes in water surface elevation. These other processes include wind forcing (set-up or set-down) within the estuary, as well as sub-tidal oscillations of the sea surface. Variations in water surface elevation can also be affected by freshwater discharge into the system, if these volumes are relatively large compared to tidal flow. The results of an analysis to determine the energy distribution (or variance) of the original water elevation time series for the Nantucket Harbor system is presented in Table V-4 compared to the energy content of the astronomical tidal signal (re-created by summing the contributions from the 23 constituents determined by the harmonic analysis). Subtracting the tidal signal from the original elevation time series resulted with the non-tidal, or residual, portion of the water elevation changes. The energy of this non-tidal signal is compared to the tidal signal, and yields a quantitative measure of how important these non-tidal physical processes can be to hydrodynamic circulation within the estuary. Figure V-10 shows the comparison of the measured tide from Nantucket Sound, with the computed astronomical tide resulting from the harmonic analysis, and the resulting non-tidal residual.

Table V-4 shows that the variance of tidal energy was essentially equal for all stations in the main basin of the system; as should be expected given the minimal tidal attenuation to the Head of the Harbor. The analysis also shows that tides are responsible for approximately 94% of the water level changes in the Nantucket Harbor system. The remaining 6% was the result of atmospheric forcing, due to winds, or barometric pressure gradients.

Table V-4. Percentages of Tidal versus Non-Tidal Energy for stations in Nantucket Harbor, September 2004.

TDR LOCATION	Total Variance (ft^2)	Tidal (%)	Non-tidal (%)
Nantucket Sound (offshore)	1.25	95.3	4.7
Brant Point	1.13	93.8	6.2
Polpis Harbor	1.13	95.0	5.0
Head of the Harbor	1.15	96.3	3.7
The Creeks	0.49	84.0	16.0
Consu Pond	0.18	74.0	26.0

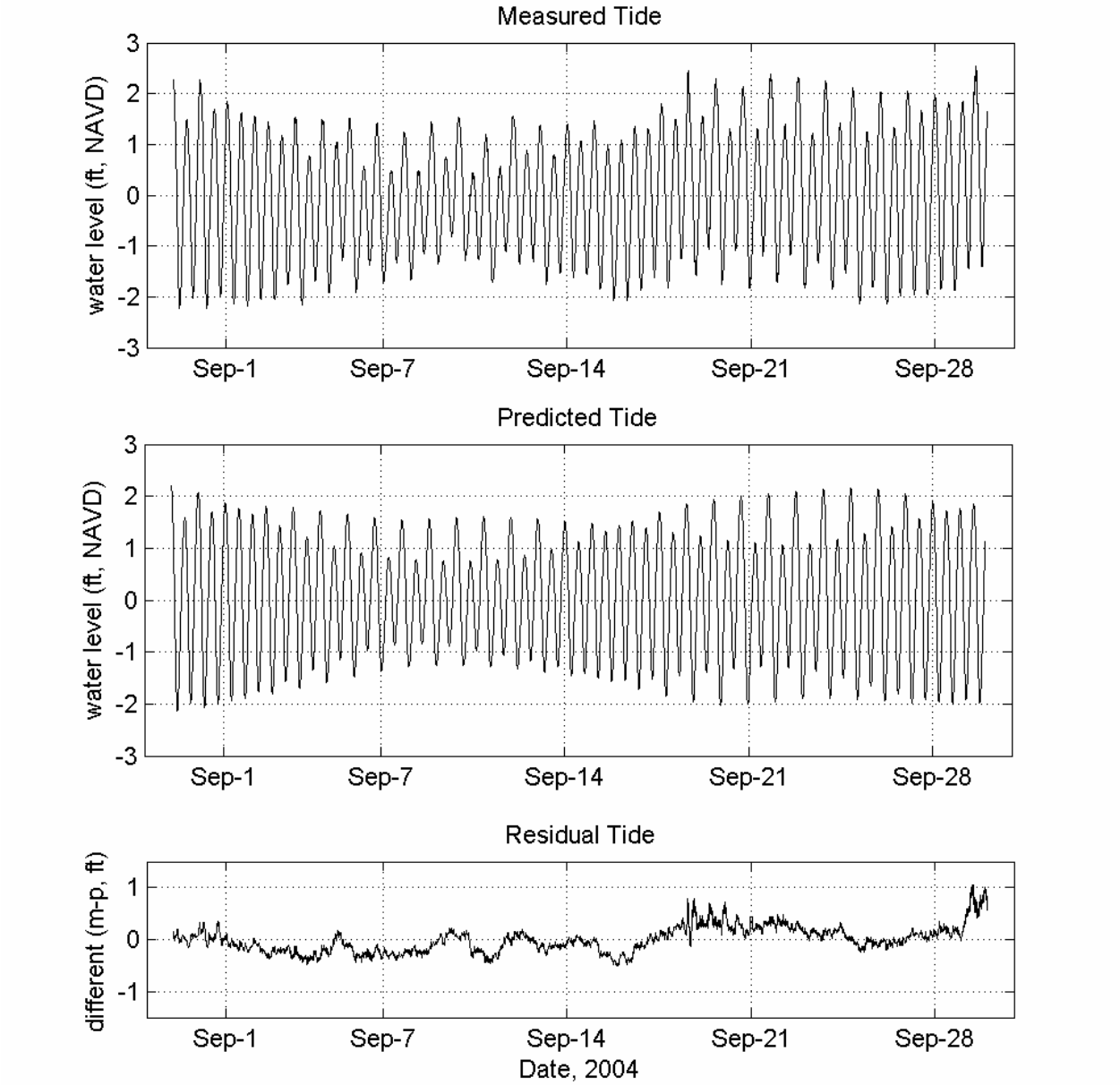

Figure V-10. Plot showing the comparison between the measured tide time series (top plot), and the predicted astronomical tide (middle plot) computed using the 23 individual tide constituents determine in the harmonic analysis of the Brant Point gauge data. The residual tide shown in the bottom plot is computed as the difference between the measured and predicted time series (r=m-p).

V.2.3 ADCP Data Analysis

Cross-channel current measurements were surveyed through a complete tidal cycle in the Nantucket Harbor system on September 23, 2004 to resolve spatial and temporal variations in tidal current patterns. The survey was designed to observe tidal flow across three transects in the system at hourly intervals. The two main transects of the survey (indicated in Figure V-5) were located 1) between Brant Point and First Point (Coatue), and 2) between first point and Shimmo (the southern Harbor shoreline). An auxiliary third transect between the tips of the inlet jetties was not followed the entire duration of the survey due to sea conditions. The data collected during this survey provided information that was necessary to model properly validate the hydrodynamic model of the Nantucket Harbor system.

Figures V-11 through V-15 show color contours of the current measurements observed during the flood and ebb tides at three of the transects. Positive along-channel currents (top panel) indicate the flow is moving into the estuary, while positive cross-channel velocities (middle panel) are oriented 90° clockwise of positive along-channel. For example, between Brant Point and First Point, positive along-channel flow is to the south, and positive cross-channel flow is moving to west. In Figure V-11, the lower left panel shows depth-averaged currents across the channel projected onto a 1994 aerial photograph of the inlet. The lower right panel of each figure indicates the stage of the tide that the survey transect was taken by a vertical line through the water elevation curve.

Between Brant Point and First Point, maximum measured currents in the water column were between 2.6 and 3.1 ft/sec (1.5 and 1.8 knots). Maximum ebb flows in the morning of the September 23 were 32,500 ft^3/sec. In the afternoon, maximum flood flows were 41,200 ft^3/sec. Across the transect between First Point and Shimmo, maximum measured currents over the entire measured tide cycle varied less, between 2.7 and 2.8 ft/sec. During maximum ebb and flood flows, the discharge rates were 28,200 ft^3/sec and 38,100 ft^3/sec, respectively.

During maximum flood, the discharge measured at the jetty tips was 19,400 ft^3/sec, which indicates that 53% of the tidal flow enters the harbor across the jetties, as opposed to between the jetty tips. This measurement indicates that the jetties are very permeable, considering that the jetties represent 88% of the flow perimeter of the inlet, with the remaining 12% being the full width of the opening between the jetty tips. Based on the percentage of the inlet flow perimeter outlined by the jetties verses the line between the jetty tips, and that 53% of the measured flow into the Nantucket Harbor flows over the jetties, the average permeability of the Nantucket jetties (i.e., average over their entire length) is computed to be 61%. The actual permeability of the jetties is dependent upon the stage of the tide.

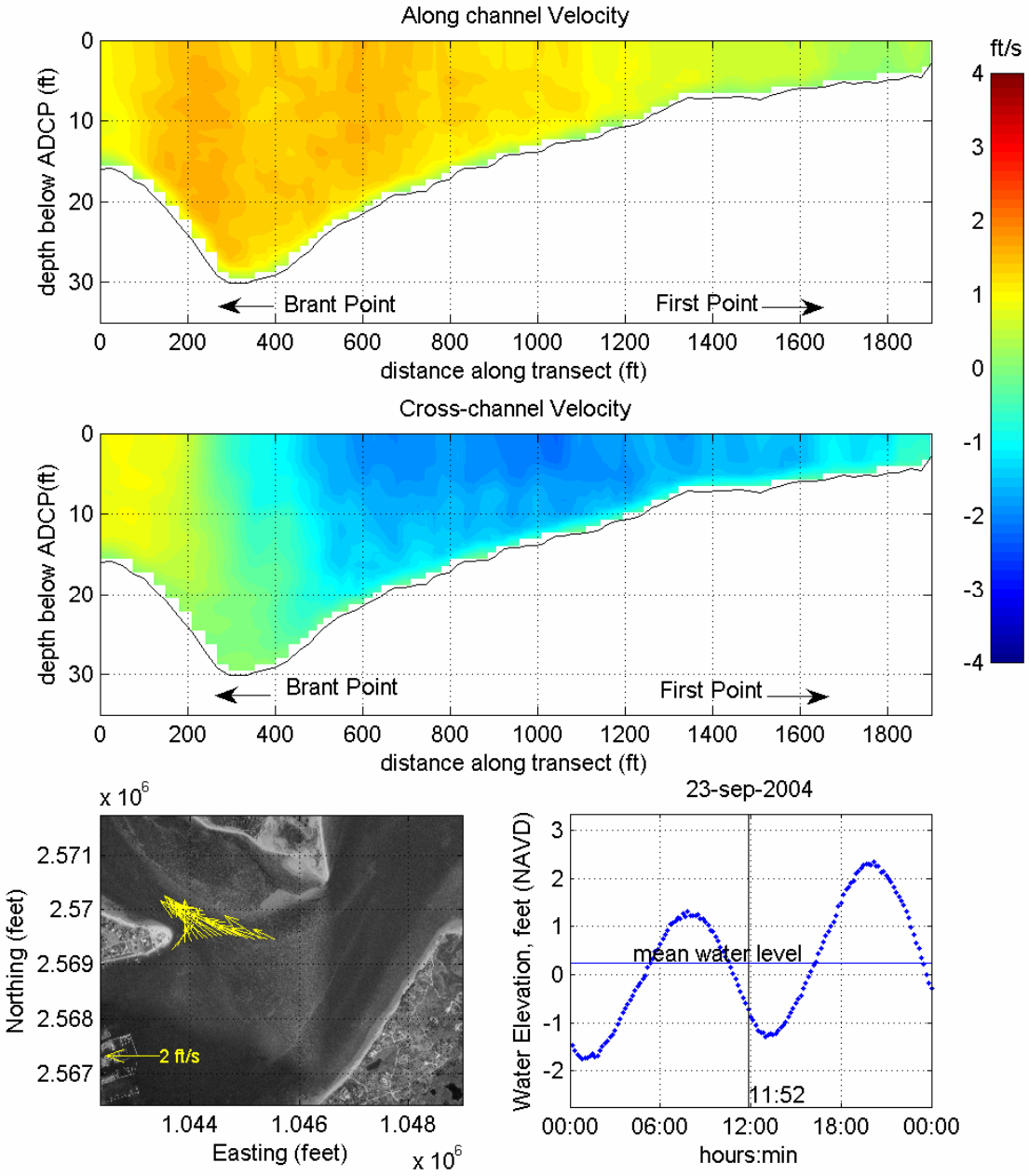

Figure V-11. Color contour plots of along-channel and cross-channel velocity components for transect line run between Brant Point and First Point, measured at 11:52 on Sep 23, 2004 during the period of maximum ebb tide currents. Positive along-channel currents (top panel) indicate the flow is moving into the estuary, while positive cross-channel velocities (middle panel) are oriented 90° clockwise of positive along-channel. Lower left plot shows scaled velocity vectors projected onto a 1994 aerial photo (MASS GIS) of the survey area. A tide plot for the survey day is also given.

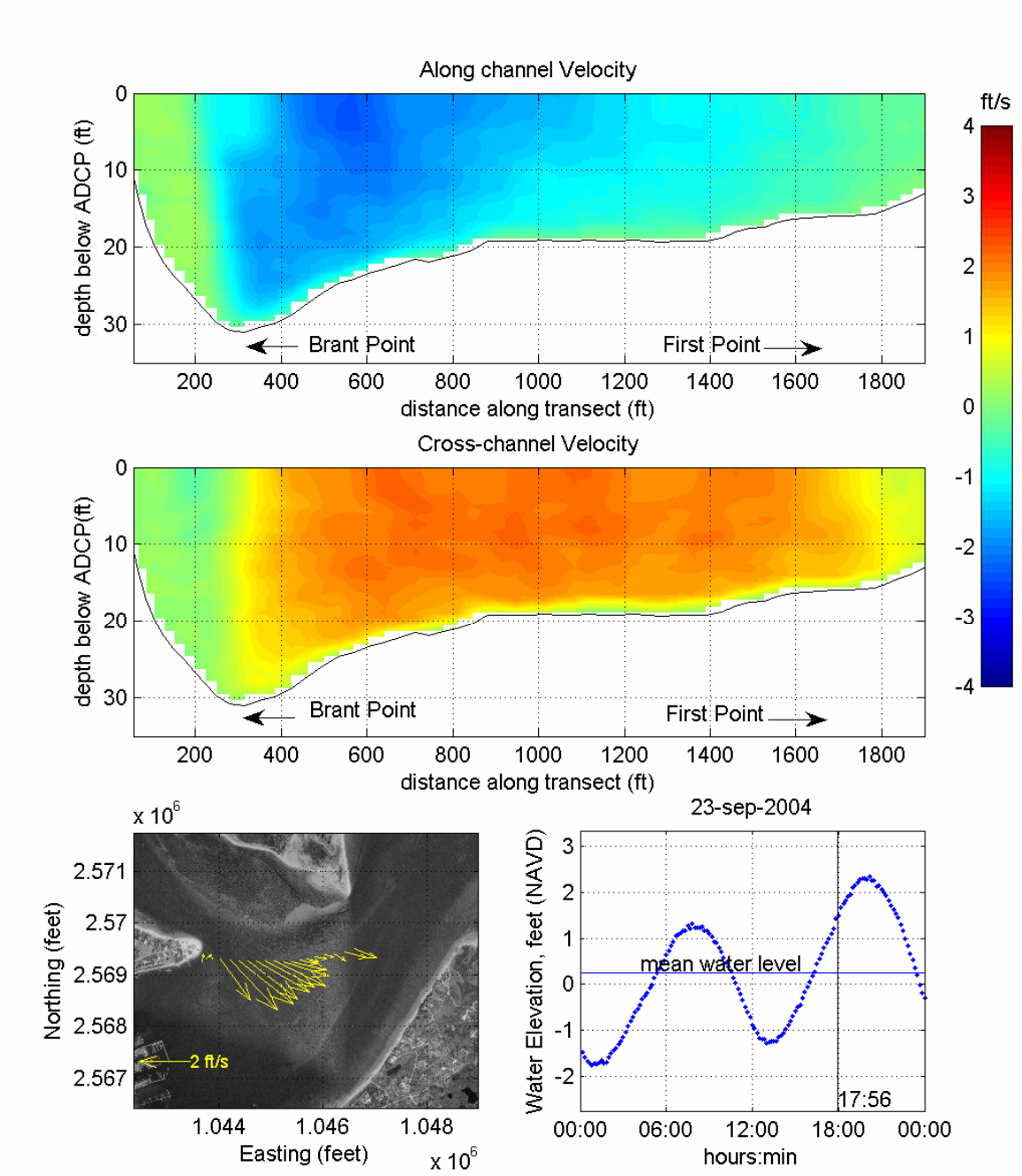

Figure V-12. Color contour plots of along-channel and cross-channel velocity components for transect line run between Brant Point and First Point, measured at 17:56 on September 23, 2004 during the period of maximum flood tide currents. Positive along-channel currents (top panel) indicate the flow is moving into the estuary, while positive cross-channel velocities (middle panel) are oriented 90° clockwise of positive along-channel. Lower left plot shows scaled velocity vectors projected onto a 1994 aerial photo (MASS GIS) of the survey area. A tide plot for the survey day is also given.

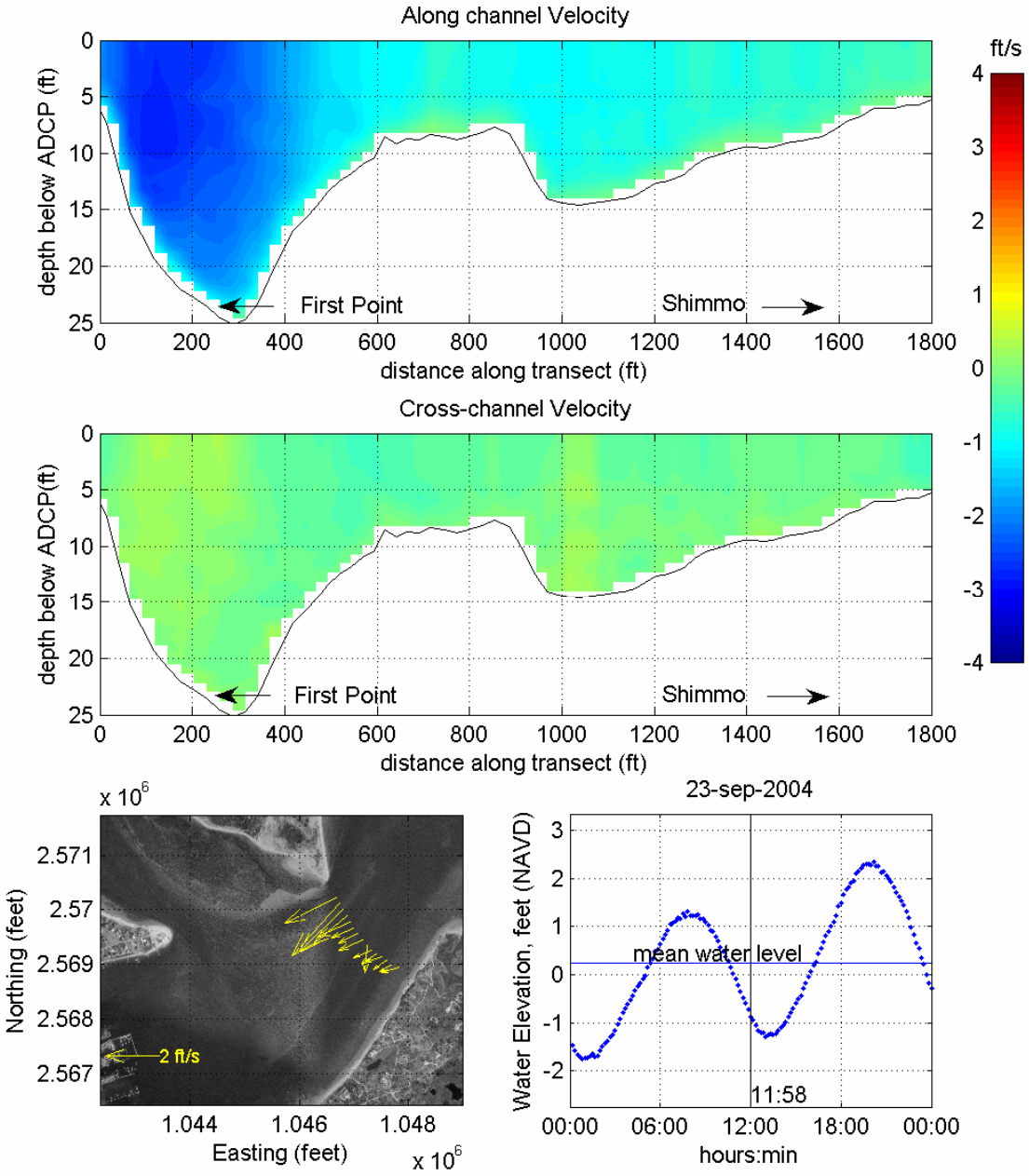

Figure V-13. Color contour plots of along-channel and cross-channel velocity components for transect line run First Point and Shimmo, measured at 11:58 on September 23, 2004 during the period of maximum ebb tide currents. Positive along-channel currents (top panel) indicate the flow is moving into the estuary, while positive cross-channel velocities (middle panel) are oriented 90° clockwise of positive along-channel. Lower left plot shows scaled velocity vectors projected onto a 1994 aerial photo (MASS GIS) of the survey area. A tide plot for the survey day is also given.

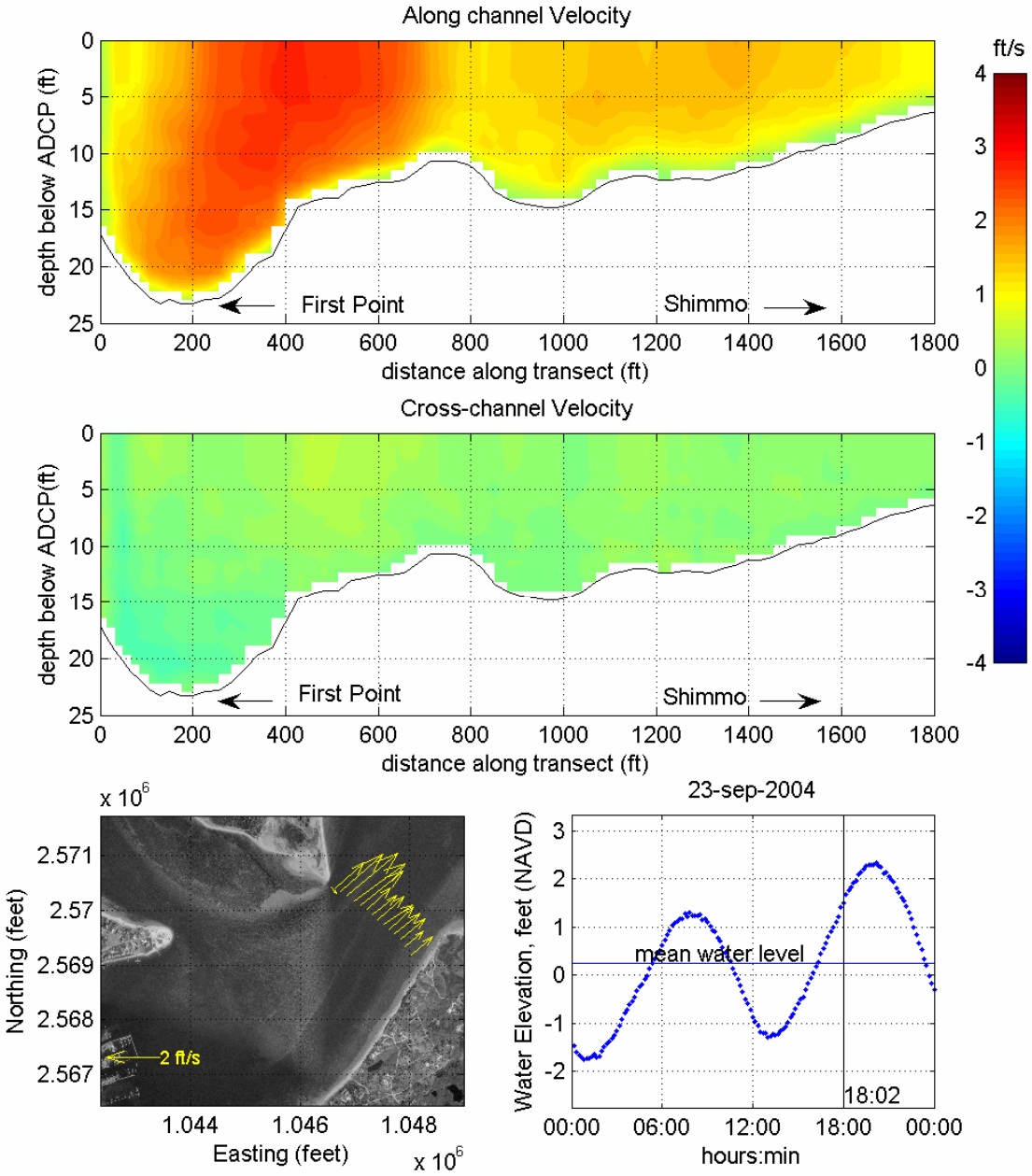

Figure V-14. Color contour plots of along-channel and cross-channel velocity components for transect line run First Point and Shimmo, measured at 18:02 on September 23, 2004 during the period of maximum flood tide currents. Positive along-channel currents (top panel) indicate the flow is moving into the estuary, while positive cross-channel velocities (middle panel) are oriented 90° clockwise of positive along-channel. Lower left plot shows scaled velocity vectors projected onto a 1994 aerial photo (MASS GIS) of the survey area. A tide plot for the survey day is also given.

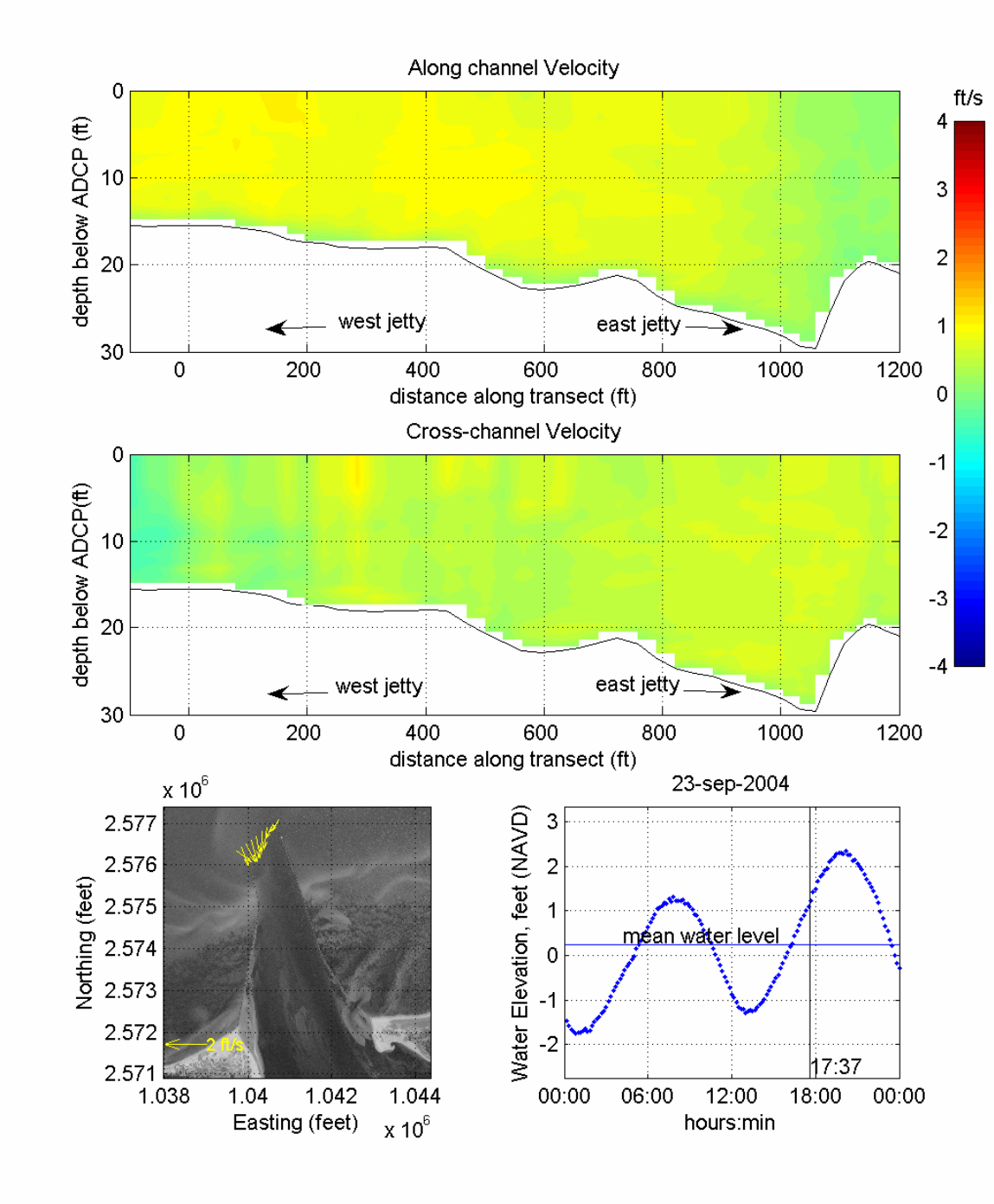

Figure V-15. Color contour plots of along-channel and cross-channel velocity components for transect line run across the jetty tips of the Harbor entrance, measured at 17:37 on September 23, 2004 during the period of maximum flood tide currents. Positive along-channel currents (top panel) indicate the flow is moving into the estuary, while positive cross-channel velocities (middle panel) are oriented 90° clockwise of positive along-channel. Lower left plot shows scaled velocity vectors projected onto a 1994 aerial photo (MASS GIS) of the survey area. A tide plot for the survey day is also given.

V.4 HYDRODYNAMIC MODELING

For modeling of Nantucket Harbor, Applied Coastal utilized a state-of-the-art computer model to evaluate tidal circulation and flushing in this system. The particular model employed was the RMA-2 model developed by Resource Management Associates (King, 1990). It is a two-dimensional, depth-averaged finite element model, capable of simulating transient hydrodynamics. The model is widely accepted and tested for analyses of estuaries or rivers. Applied Coastal staff members have utilized RMA-2 for numerous flushing studies on Cape Cod and the Islands, including West Falmouth Harbor, Popponesset Bay, Pleasant Bay (Howes, *et al*, 2006), Falmouth "finger" Ponds (Ramsey, *et al*, 2000), and Barnstable Harbor (Wood, *et al*, 1999), and Three Bays (Howes, *et al*, 2005).

V.4.1 Model Theory

In its original form, RMA-2 was developed by William Norton and Ian King under contract with the U.S. Army Corps of Engineers (Norton et al., 1973). Further development included the introduction of one-dimensional elements, state-of-the-art pre- and post-processing data programs, and the use of elements with curved borders. Recently, the graphic pre- and post-processing routines were updated by a Brigham Young University through a package called the Surfacewater Modeling System or SMS (BYU, 1998). Graphics generated in support of this report primarily were generated within the SMS modeling package.

RMA-2 is a finite element model designed for simulating one- and two-dimensional depth-averaged hydrodynamic systems. The dependent variables are velocity and water depth, and the equations solved are the depth-averaged Navier Stokes equations. Reynolds assumptions are incorporated as an eddy viscosity effect to represent turbulent energy losses. Other terms in the governing equations permit friction losses (approximated either by a Chezy or Manning formulation), Coriolis effects, and surface wind stresses. All the coefficients associated with these terms may vary from element to element. The model utilizes quadrilaterals and triangles to represent the prototype system. Element boundaries may either be curved or straight.

The time dependence of the governing equations is incorporated within the solution technique needed to solve the set of simultaneous equations. This technique is implicit; therefore, unconditionally stable. Once the equations are solved, corrections to the initial estimate of velocity and water elevation are employed, and the equations are re-solved until the convergence criteria is met.

V.4.2 Model Setup

There are three main steps required to implement RMA-2:

- Grid generation
- Boundary condition specification
- Calibration

The extent of each finite element grid was generated using 2003 color digital aerial photographs from the MassGIS online orthophoto database. A time-varying water surface elevation boundary condition (measured tide) was specified at the inlet of the Harbor system based on the tide gauge data collected offshore Coatue, in Nantucket Sound. Once the grid and boundary conditions were set, the model was calibrated to ensure accurate predictions of tidal flushing. Various friction and eddy viscosity coefficients were adjusted, through several model calibration simulations for the system, to obtain agreement between measured and

modeled tides. The calibrated model provides the requisite information for future detailed water quality modeling.

V.4.2.1 Grid generation

The grid generation process was aided by the use of the SMS package. 2003 digital aerial orthophotos and recent bathymetry survey data were imported to SMS, and a finite element grid was created to represent the estuary. The aerial photographs were used to determine the land boundary of the system. Bathymetry data were interpolated to the developed finite element mesh of the system. The completed grid consists of 7,006 nodes, which describe 2,647 total 2-dimensional (depth averaged) quadratic elements, and covers 8,860 acres. The maximum nodal depth is -41.4 ft (NAVD 88) in the included offshore area of the grid, and -28.3 within the Harbor basin. The completed grid mesh of the Nantucket system is shown in Figure V-16, and grid bathymetry was shown previously in Figure V-6.

The finite element grid for the system provided the detail necessary to evaluate accurately the variation in hydrodynamic properties throughout the Harbor. The SMS grid generation program was used to develop quadrilateral and triangular two-dimensional elements throughout the estuary. Grid resolution was governed by two factors: 1) expected flow patterns, and 2) the bathymetric variability of the system. Relatively fine grid resolution was employed where complex flow patterns were expected. For example, smaller node spacing in main and sub-systems inlet channels was designed to provide a more detailed analysis in these regions of rapidly varying flow (e.g., the inlet channel and Polpis Harbor). Widely spaced nodes were often employed in areas where flow patterns are not likely to change dramatically, such as in the main bodies of the harbor, such as the Head of the Harbor. Appropriate implementation of wider node spacing and larger elements was used to reduce computer run time with no sacrifice of accuracy.

V.4.2.2 Boundary condition specification

Two types of boundary conditions were employed for the RMA-2 model of the Nantucket Harbor system: 1) "slip" boundaries, and 2) tidal elevation boundaries. All of the elements with land borders have "slip" boundary conditions, where the direction of flow was constrained shore-parallel. The model generated all internal boundary conditions from the governing conservation equations. Tidal boundary conditions were specified at the inlet from Nantucket Sound. TDR measurements from a gauge deployed offshore Coatue provided the required data.

The rise and fall of the tide in Nantucket Sound is the primary driving force for estuarine circulation in this system. Dynamic (time-varying) model simulations specified a new water surface elevation at the model's offshore open boundary every model time step of 10 minutes, which corresponds to the time step of the TDR data measurements.

V.4.2.3 Calibration

After developing the finite element grid, and specifying boundary conditions, the model for the Nantucket Harbor system was calibrated. The calibration procedure ensures that the model predicts accurately what was observed in nature during the field measurement program. Numerous model simulations are required (typically 10+) for an estuary model, specifying a range of friction and eddy viscosity coefficients, to calibrate the model.

Calibration of the hydrodynamic model required a close match between the modeled and measured tides in each of the sub-embayments where tides were measured (i.e., from the TDR

deployments). Initially, the model was calibrated to obtain visual agreement between modeled and measured tides. Once visual agreement was achieved, a five lunar-day period (10 tide cycles) was modeled to calibrate the model based on dominant tidal constituents discussed in Section V.3.2. The five-day period was extracted from a longer simulation to avoid effects of model spin-up, and to focus on average tidal conditions. Modeled tides for the calibration time period were evaluated for time (phase) lag and height damping of dominant tidal constituents.

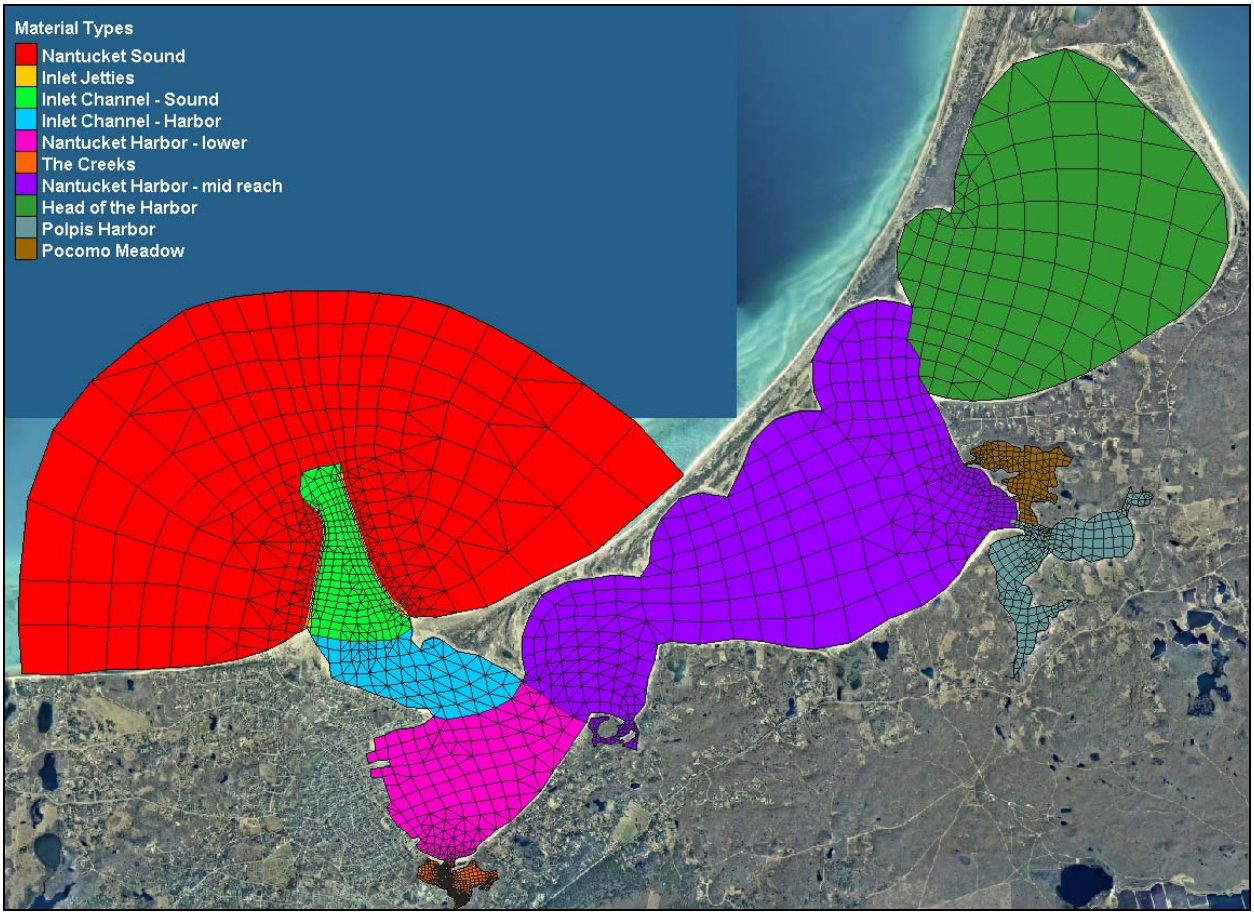

Figure V-16. Plot of hydrodynamic model grid mesh for the Nantucket Harbor estuarine system of Nantucket Island, Massachusetts. Color patterns designate the different model material types used to vary model calibration parameters and compute flushing rates.

The calibration was performed for a five-day period beginning August 30, 2004 at 0000 EDT. This representative time period included the spring tide range of conditions, where the tide range and tidal currents are greatest, and model numerical stability is often most sensitive. To provide average tidal forcing conditions for model verification and the flushing analysis, a separate time period was chosen that spanned the transition between spring and neap tide ranges (bi-weekly maximum and minimum tidal ranges, respectively).

The calibrated model was used to analyze system flow patterns and compute residence times. The ability to model a range of flow conditions is a primary advantage of a numerical tidal flushing model. For instance, average residence times were computed using the entire seven-day simulation. Other methods, such as dye and salinity studies, evaluate tidal flushing over relatively short time periods (less than one day). These short-term measurement

techniques may not be representative of average conditions due to the influence of unique, short-lived atmospheric events.

V.4.2.3.1 Friction coefficients

Friction inhibits flow along the bottom of estuary channels or other flow regions where velocities are relatively high. Friction is a measure of the channel roughness, and can cause both significant amplitude damping and phase delay of the tidal signal. Friction is approximated in RMA-2 as a Manning coefficient, and is applied to grid areas by user specified material types. Initially, Manning's friction coefficient values of 0.025 were specified for all element material types. This values corresponds to typical Manning's coefficients determined experimentally in smooth earth-lined channels with no weeds (low friction) (Henderson, 1966).

During calibration, friction coefficients were incrementally changed throughout the model domain. Final model calibration runs incorporated various specific values for Manning's friction coefficients, depending upon flow damping characteristics of separate regions within the estuary system. Manning's values for different bottom types were initially selected based ranges provided by the Civil Engineering Reference Manual (Lindeburg, 1992), and values were incrementally changed when necessary to obtain a close match between measured and modeled tides. Final calibrated friction coefficients are summarized in the Table V-5.

Table V-5. Manning's Roughness coefficients used in simulations of modeled sub-embayments. These embayment delineations correspond to the material type areas shown in Figure V-16.

System Embayment	Bottom Friction
Nantucket Sound	0.025
Inlet Jetties	0.100
Inlet Channel - Sound	0.025
Inlet Channel - Harbor	0.025
Nantucket Harbor - Lower	0.025
The Creeks	0.070
Nantucket Harbor - Mid Reach	0.040
Head of the Harbor	0.025
Polpis Harbor	0.025
Pomoco Meadow	0.070

V.4.2.3.2 Turbulent exchange coefficients

Turbulent exchange coefficients approximate energy losses due to internal friction between fluid particles. The significance of turbulent energy losses increases where flow is swifter, such as inlets and other channel constrictions. According to King (1990), these values are proportional to element dimensions (numerical effects) and flow velocities (physics). Typically, model turbulence coefficients were set between 80 and 300 lb-sec/ft^2. In most cases, the Nantucket Harbor system was relatively insensitive to turbulent exchange coefficients. The exception was at the inlets, where higher exchange coefficient values (300 lb-sec/ft^2) were used to ensure numerical stability in these areas characterized by strong turbulent flows and large velocity magnitudes.

V.4.2.3.3 Marsh porosity processes

Modeled hydrodynamics were complicated by wetting/drying cycles on the marsh plain regions included in the model of the Nantucket Harbor system. Cyclically wet/dry areas of the marsh will tend to store waters as the tide begins to ebb and then slowly release water as the water level drops within the creeks and channels. This store-and-release characteristic of these marsh regions was partially responsible for the distortion of the tidal signal, and the elongation of the ebb phase of the tide. On the flood phase, water rises within the channels and creeks initially until water surface elevation reaches the marsh plain, when at this point the water level remains nearly constant as water 'fans' out over the marsh surface. The rapid flooding of the marsh surface corresponds to a flattening out of the tide curve approaching high water. Marsh porosity is a feature of the RMA-2 model that permits the modeling of hydrodynamics in marshes. This model feature essentially simulates the store-and-release capability of the marsh plain by allowing grid elements to transition gradually between wet and dry states. This technique allows RMA-2 to change the ability of an element to hold water, like squeezing a sponge.

V.4.2.3.4 Comparison of modeled tides and measured tide data

A best-fit of model predictions for the TDR deployment was achieved using the aforementioned values for friction and turbulent exchange. Figures V-17 through and V-20 illustrate the five-day calibration simulation along with a 50-hour sub-section. Modeled (solid line) and measured (dotted line) tides are illustrated at each model location with a corresponding TDR.

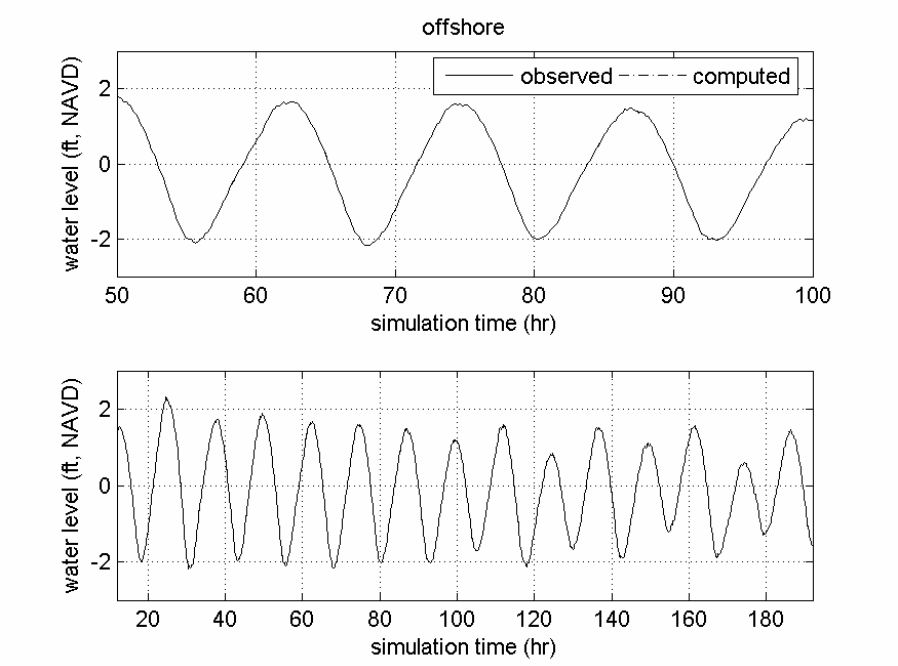

Figure V-17. Comparison of model output and measured tides for the TDR location offshore the inlet to Nantucket Harbor, in Nantucket Sound. The top plot is a 50-hour sub-section of the total modeled time period, shown in the bottom plot.

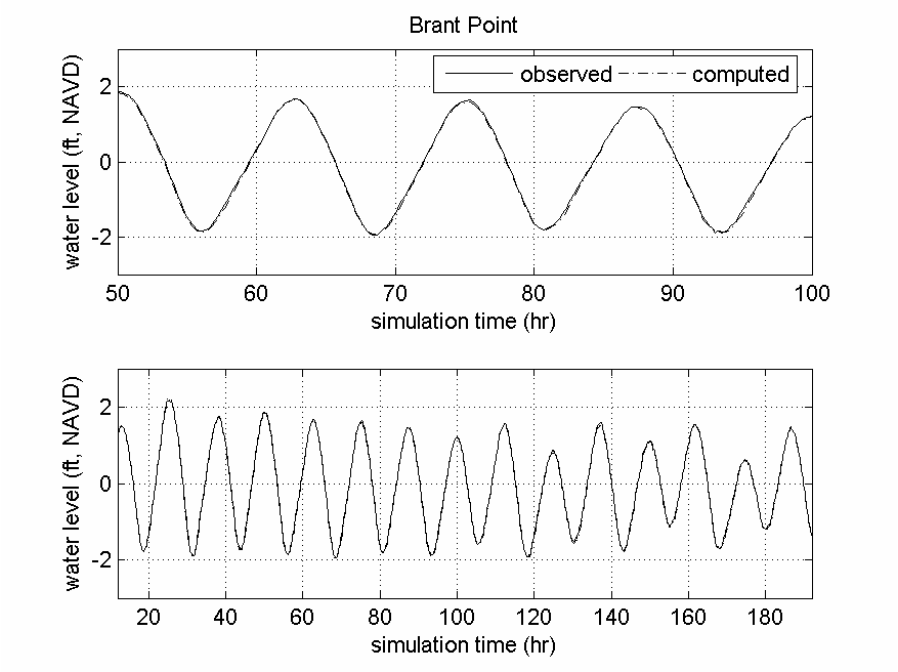

Figure V-18. Comparison of model output and measured tides for the TDR location at Brant Point. The top plot is a 50-hour sub-section of the total modeled time period, shown in the bottom plot.

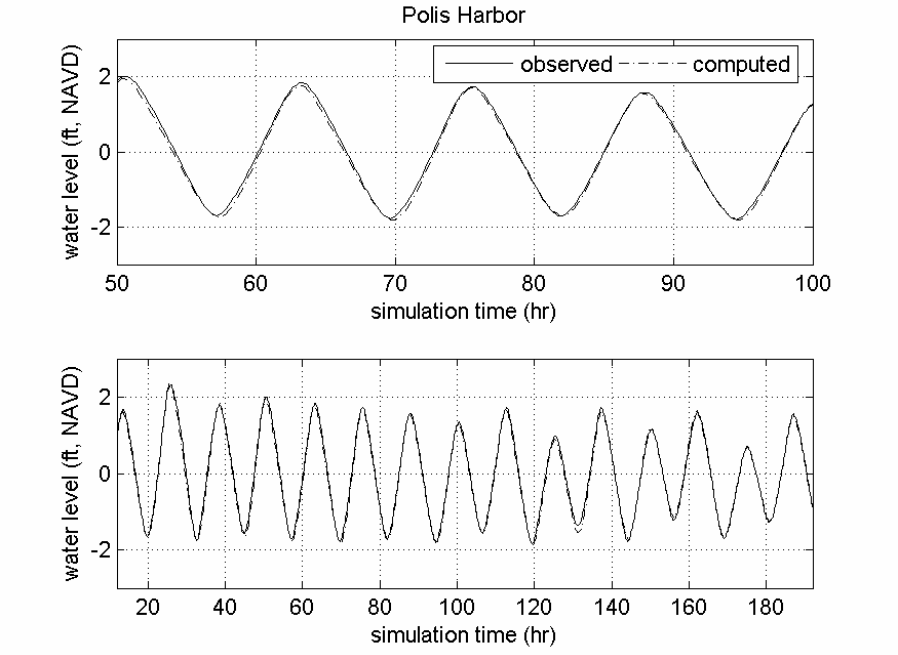

Figure V-19. Comparison of model output and measured tides for the TDR location in Polpis Harbor. The top plot is a 50-hour sub-section of the total modeled time period, shown in the bottom plot.

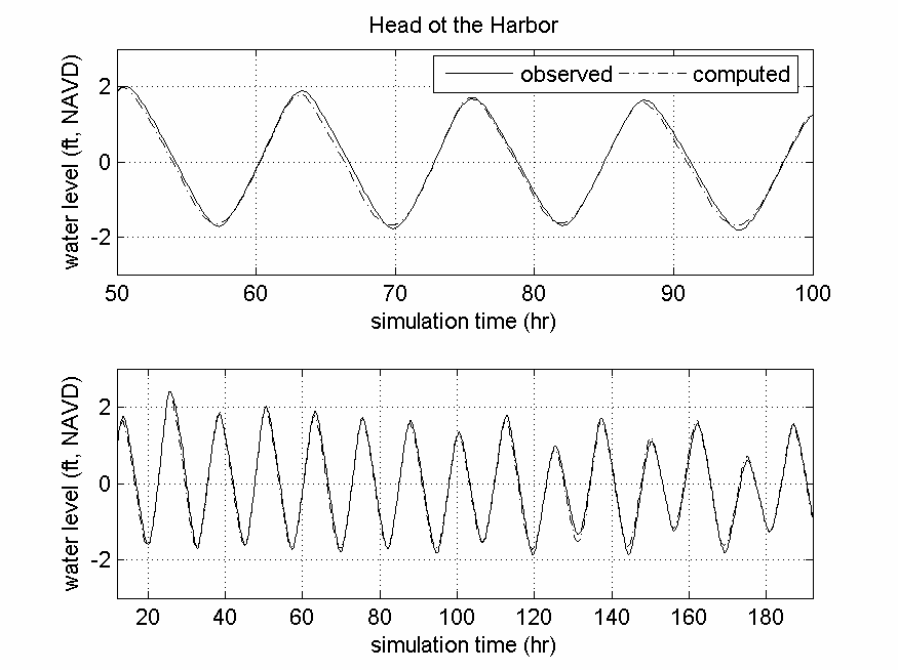

Figure V-20. Comparison of model output and measured tides for the TDR location at the Head of the Harbor. The top plot is a 50-hour sub-section of the total modeled time period, shown in the bottom plot.

Although visual calibration achieved reasonable modeled tidal hydrodynamics, further tidal constituent calibration was required to quantify the accuracy of the models. Calibration of M_2 (principle lunar semidiurnal constituent) was the highest priority since M_2 accounted for a majority of the forcing tide energy in the modeled system. Due to the duration of the model runs, four dominant tidal constituents were selected for constituent comparison: K_1, M_2, M_4, and M_6. Measured tidal constituent heights (H) and time lags (ϕ_{lag}) shown in Table V-6 for the calibration period differ from those in Table V-2 because constituents were computed for only the five-day section of the 31-days represented in Table V-2. Table V-6 compares tidal constituent amplitude (height) and relative phase (time) for modeled and measured tides at the TDR locations. The constituent phase shows the relative timing of each separate constituent at a particular location, and also the change (or phase lag) in timing of a single constituent at different locations in an estuary.

he constituent calibration resulted in excellent agreement between modeled and measured tides. The largest errors associated with tidal constituent amplitude were on the order of 0.01 ft, which is better than the order of accuracy of the tide gauges (±0.12 ft). Time lag errors were typically less than the time increment resolved by the model (1/6 hours or 10 minutes), indicating good agreement between the model and data.

Table V-6. Tidal constituents for measured water level data and calibrated model output, with model error amplitudes, for the Nantucket Harbor system, during modeled calibration time period.

Model calibration run						
Location	Constituent Amplitude (ft)				Phase (deg)	
	M_2	M_4	M_6	K_1	ϕM_2	ϕM_4
Nantucket Sound*	1.71	0.15	0.06	0.09	29.2	179.4
Brant Point	1.63	0.09	0.05	0.09	41.3	-177.5
Polpis Harbor	1.59	0.11	0.06	0.08	63.0	56.1
Head of the Harbor	1.58	0.09	0.07	0.08	61.9	68.3
Measured tide during calibration period						
Location	Constituent Amplitude (ft)				Phase (deg)	
	M_2	M_4	M_6	K_1	ϕM_2	ϕM_4
Nantucket Sound*	1.71	0.15	0.06	0.08	30.6	-176.4
Brant Point	1.61	0.11	0.06	0.08	42.7	-170.2
Polpis Harbor	1.59	0.06	0.07	0.08	64.2	47.9
Head of the Harbor	1.60	0.09	0.07	0.11	66.7	51.4
Error						
Location	Error Amplitude (ft)				Phase error (min)	
	M_2	M_4	M_6	K_1	ϕM_2	ϕM_4
Nantucket Sound*	0.00	0.00	0.00	-0.01	2.9	4.4
Brant Point	-0.02	0.02	0.01	-0.01	2.8	7.6
Polpis Harbor	0.00	-0.05	0.01	0.00	2.6	-8.5
Head of the Harbor	0.02	0.00	0.00	0.02	9.9	-17.6

*model open boundary

V.4.2.4 ADCP verification of the Nantucket Harbor system

An additional model verification check was possible by using collected ADCP velocity data to verify the performance of the Nantucket Harbor system model. Computed flow rates from the model were compared to flow rates determined using the measured velocity data. The ADCP data survey efforts are described in Section 2. For the model ADCP verification, the Harbor model was run for the period covered during the ADCP survey on September 23, 2004. Model flow rates were computed in RMA-2 at continuity lines (channel cross-sections) that correspond to two of the actual ADCP transects followed in each survey (i.e., between Brant Point and First Point, and between First Point and Shimmo). The ADCP transect between the two jetty tips was not used for the model verification because there are not sufficient measurements from this transect to make a useful comparison to model output.

Comparisons of the measured and modeled volume flow rates in the Nantucket Harbor system are shown in Figures V-21 and V-22. For each figure, the top plot shows the flow comparison, and the lower plot shows the time series of tide elevation for the same period. Each ADCP point (blue triangles shown on the plots) is a summation of flow measured along the ADCP transect. The 'bumps' and 'skips' of the flow rate curve (more evident in the model output) can be attributed to the effects of winds (i.e., atmospheric effects) on the water surface and friction across the seabed periodically retarding or accelerating the flow through the inlets, and inside the system channels. If water surface elevations changed smoothly as a sinusoid, the volume flow rate would also appear as a smooth curve. However, since the rate at which water surface elevations change does not vary smoothly, the flow rate curve is expected to show short-period fluctuations.

Data comparisons at all five ADCP transect show exceptionally good agreement with the model predictions. The calibrated model accurately describes the discharge magnitude at both lines. For all transects the R^2 correlation coefficients between data and model results are equal or greater than 0.98. The RMS error computed from each transect is less than 3,200 ft3/sec, which is 6.8% of the maximum measured discharge rate. Correlation statistics between the modeled and measured flows for each ADCP transect are presented in Table V-7.

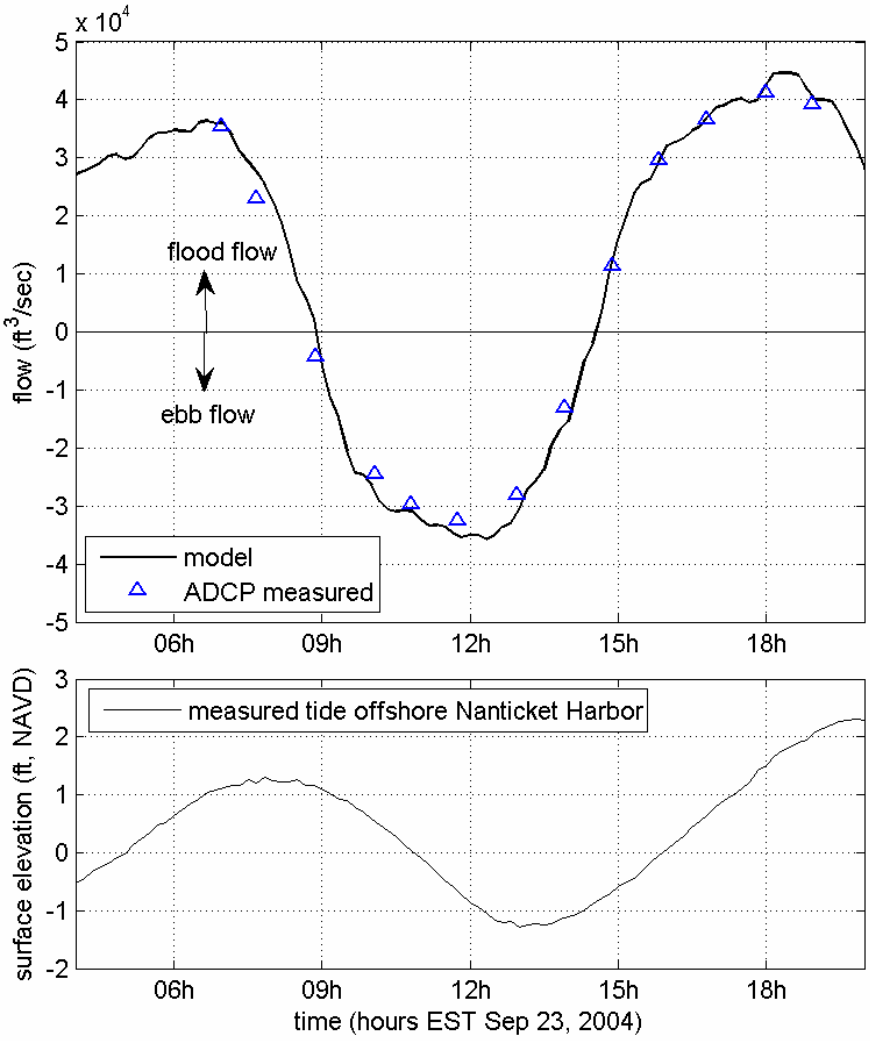

Figure V-21. Comparison of measured volume flow rates versus modeled flow rates (top plot) through the Nantucket Harbor Inlet between Brant Point and First Point, over a tidal cycle on September 23, 2004. Flood flows into the inlet are positive (+), and ebb flows out of the inlet are negative (-). The bottom plot shows the tide elevation offshore the Harbor Inlet. (R^2 =0.99, E_{RMS}=3,100 ft^3/sec).

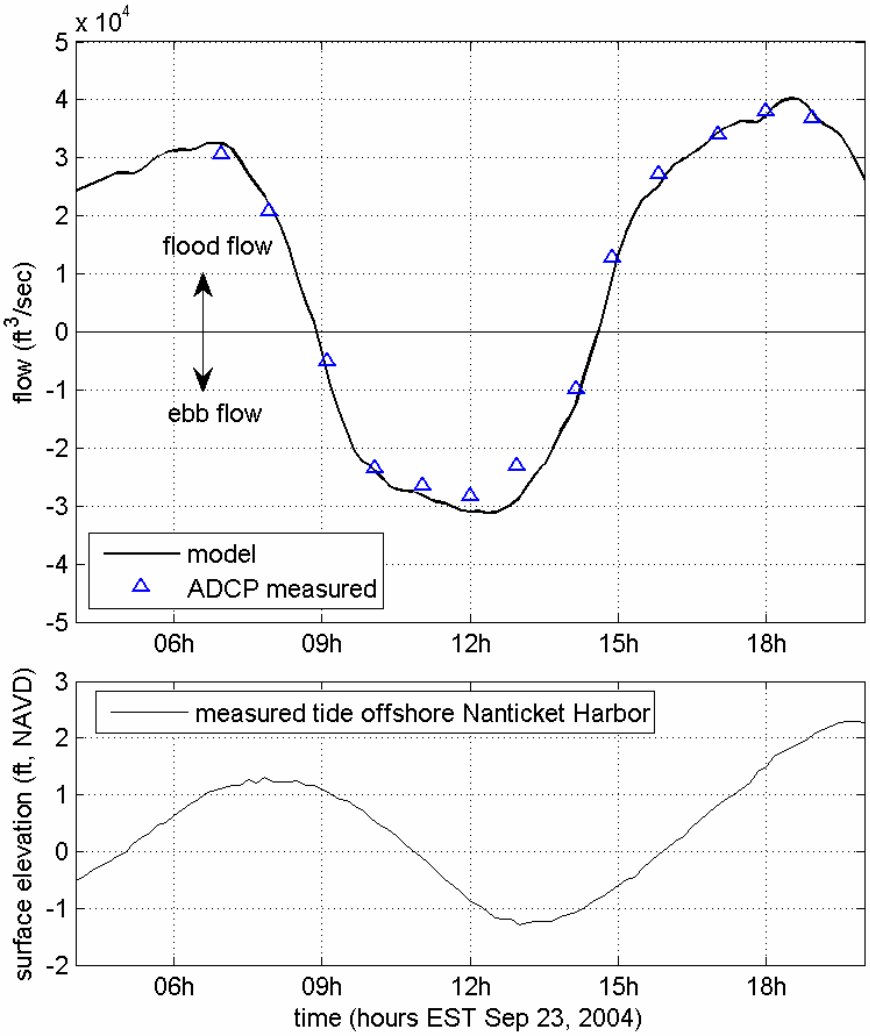

Figure V-22. Comparison of measured volume flow rates versus modeled flow rates (top plot) in Nantucket Harbor between First Point and Shimmo, over a tidal cycle on September 23, 2004. Flood flows into the inlet are positive (+), and ebb flows out of the inlet are negative (-). The bottom plot shows the tide elevation offshore the Harbor inlet. (R^2=0.98, E_{RMS}=3,200 ft^3/sec).

Table V-7. Correlation statistics between modeled and measured total flow rates at the ADCP transects used in the model verification of the Nantucket Harbor model.

Transect	R^2 correlation	RMS error (ft^3/sec)	Max Error (ft^3/sec)	Min Error (ft^3/sec)
Brant Point to First Point	0.99	3,100	6,500	400
First Point to Shimmo	0.98	3,200	6,700	200

V.4.2.6 Model Circulation Characteristics

The final calibrated model serves as a useful tool in investigating the circulation characteristics of the Nantucket Harbor system. Using model inputs of bathymetry and tide

data, current velocities and flow rates can be determined at any point in the model domain. This is a very useful feature of a hydrodynamic model, where a limited amount of collected data can be expanded to determine the physical attributes of the system in areas where no physical data record exists.

From the model run of the Harbor, maximum ebb velocities in the inlet channels are slightly larger than velocities during maximum flood. Maximum depth-averaged flood velocities in the model are approximately 2.4 feet/sec near First Point, while maximum ebb velocities are about 3.9 feet/sec. Close-up views of model output are presented in Figure V-23 and V-24, which show contours of velocity magnitude along with velocity vectors that indicate flow direction, each for a single model time-step, at the portion of the tide where maximum ebb velocities occur (in Figure V-23), and for maximum flood velocities in Figure V-24.

In addition to depth-averaged velocities, the total flow rate of water flowing through a channel can be computed with the hydrodynamic model. The variation of flow as the tide floods and ebbs at the two system inlets is seen in the plot of flow rates in Figure V-25. Maximum flow rates occur during ebbing tides in this system. During spring tides, the maximum flood flow rates reach 50,600 ft^3/sec at the Harbor entrance between Brant Point and First Point. Maximum ebb flow rates during spring tides are slightly greater between Brant Point and First Point, about 51,900 ft^3/sec. Minimum flood flows at the Harbor Entrance during neap tides are 30,400 ft^3/sec, and minimum ebb flows during neap tides are approximately 27,500 ft^3/sec.

Another feature of the Nantucket Harbor system model is a persistent tidal eddy (or gyre) in the main commercial basin of the Harbor (near the village of Nantucket) which is set-up during flooding tides. The eddy can be seen in model output shown in Figure V-26, to the south of Brant Point. The eddy has a faint clock-wise rotation, with velocity magnitudes that are less than 0.25 ft/sec.

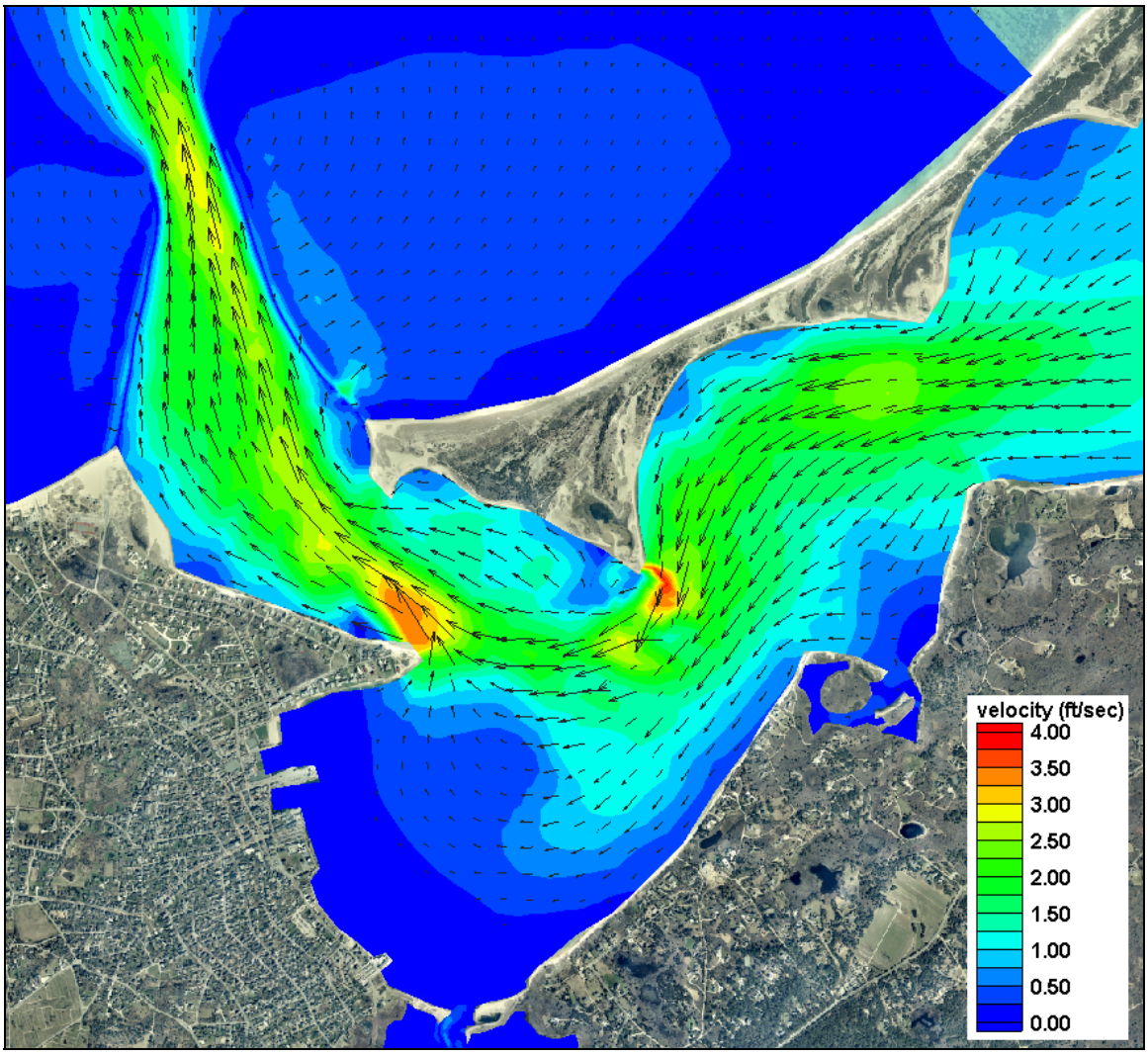

Figure V-23. Example of hydrodynamic model output for a single time step where maximum ebb velocities occur for this tide cycle. Color contours indicate velocity magnitude, and vectors indicate the direction of flow.

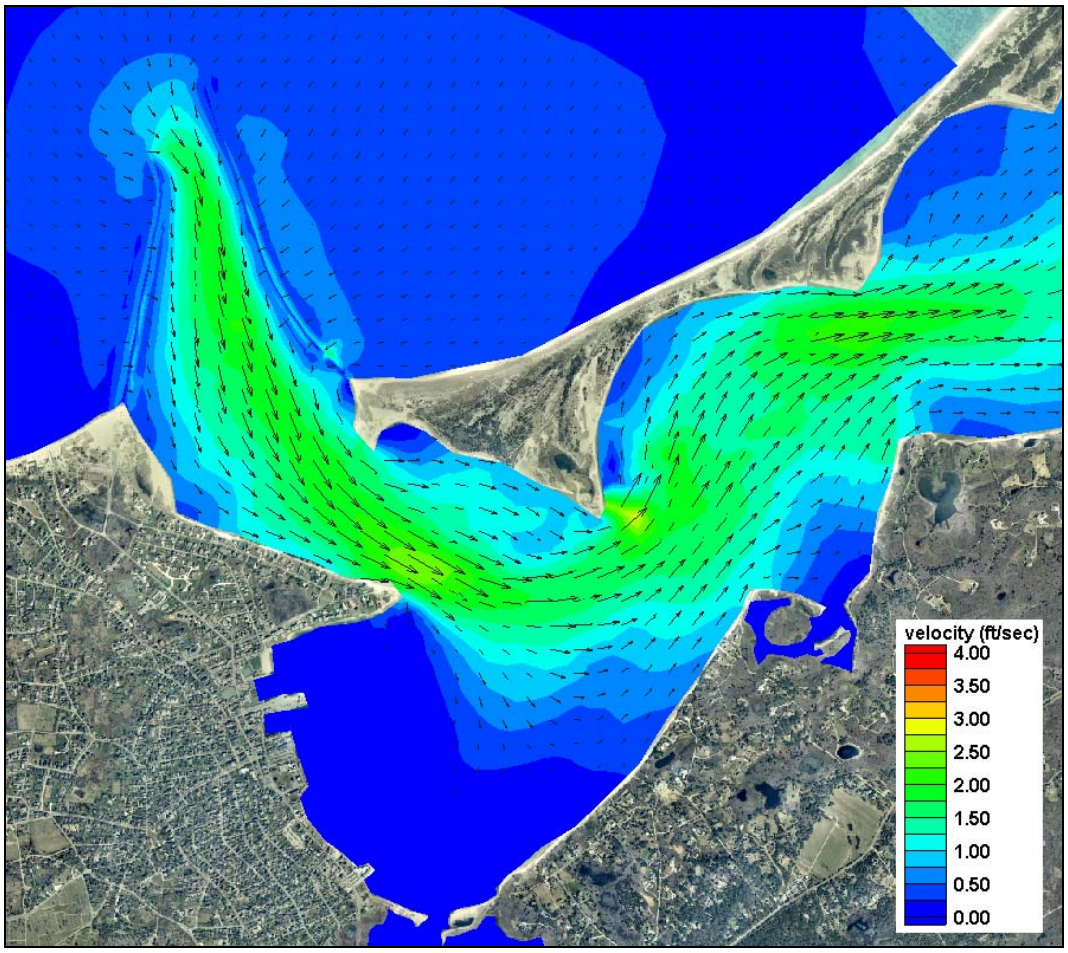

Figure V-24. Example of hydrodynamic model output for a single time step where maximum ebb velocities occur for this tide cycle. Color contours indicate velocity magnitude, and vectors indicate the direction of flow.

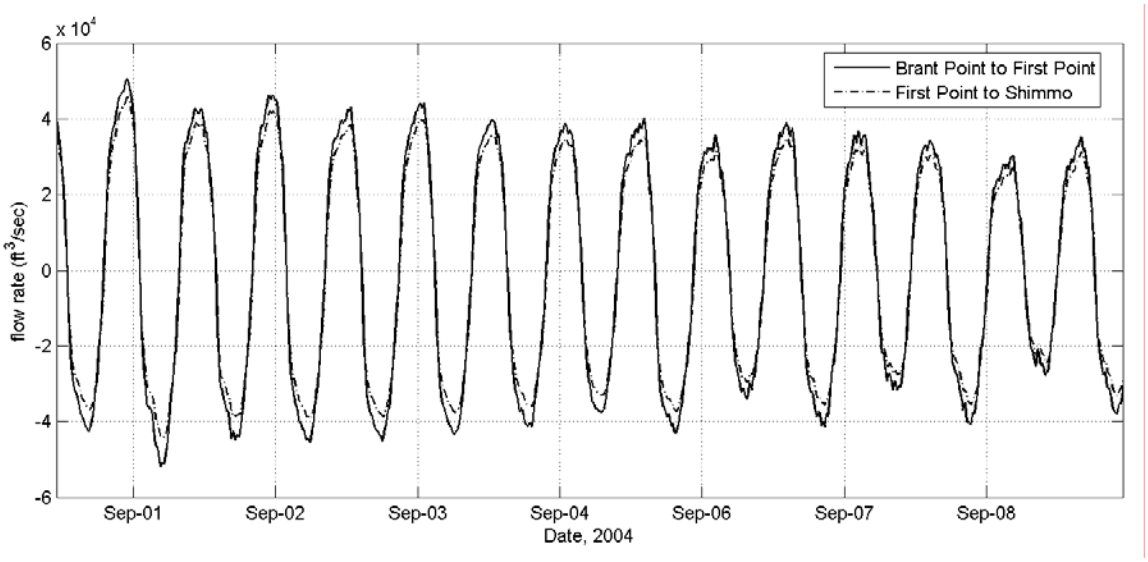

Figure V-25. Time variation of computed flow rates at two channel transects in the Nantucket Harbor system. Positive flow indicated flooding tide, while negative flow indicates ebbing tide.

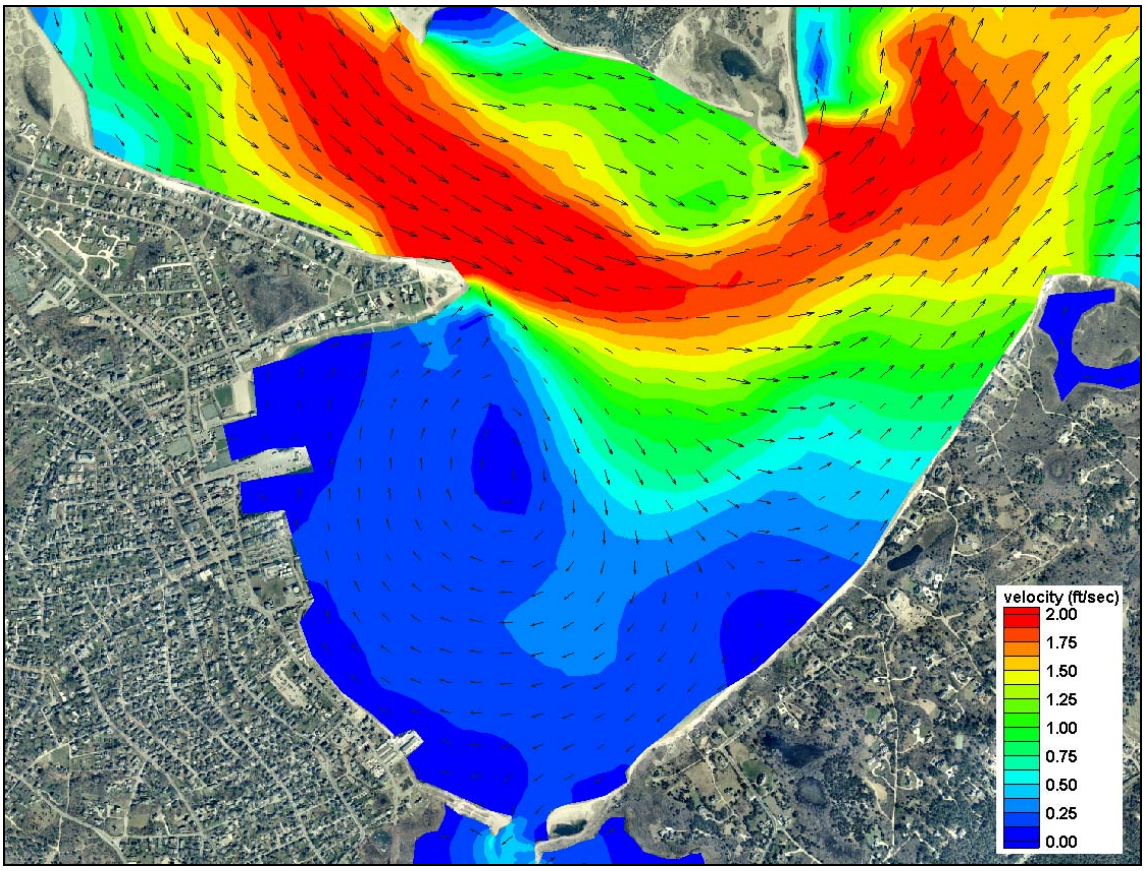

Figure V-26. Close-up of Nantucket Harbor, showing output from the hydrodynamic model at a single time step, where a recirculation eddy (or gyre) has set up on the south side of Brant Point.

V.5 FLUSHING CHARACTERISTICS

Since the magnitude of freshwater inflow is much smaller in comparison to the tidal exchange through each inlet, the primary mechanism controlling estuarine water quality within the modeled Nantucket Harbor system is tidal exchange. A rising tide offshore in Nantucket Sound creates a slope in water surface from the ocean into the upper-most reaches of the modeled system. Consequently, water flows into (floods) the system. Similarly, the estuary drains into the open waters of Nantucket Sound on an ebbing tide. This exchange of water between the system and the ocean is defined as tidal flushing. The calibrated hydrodynamic model is a tool to evaluate quantitatively tidal flushing of the Harbor system, and was used to compute flushing rates (residence times) and tidal circulation patterns.

Flushing rate, or residence time, is defined as the average time required for a parcel of water to migrate out of an estuary from points within the system. For this study, **system residence times** were computed as the average time required for a water parcel to migrate from a point within the each embayment to the entrance of the system. System residence times are computed as follows:

$$T_{system} = \frac{V_{system}}{P} t_{cycle}$$

where T_{system} denotes the residence time for the system, V_{system} represents volume of the (entire) system at mean tide level, P equals the tidal prism (or volume entering the system through a single tidal cycle), and t_{cycle} the period of the tidal cycle, typically 12.42 hours (or 0.52 days). To compute system residence time for a sub-embayment, the tidal prism of the sub-embayment replaces the total system tidal prism value in the above equation.

In addition to system residence times, a second residence, the **local residence time**, was defined as the average time required for a water parcel to migrate from a location within a sub-embayment to a point outside the sub-embayment. Using Polpis Harbor as an example, the **system residence time** is the average time required for water to migrate from Polpis Harbor, through the mid-reach of Nantucket Harbor, out through the inlet, and into Nantucket Sound, where the **local residence time** is the average time required for water to migrate from Polpis Harbor to just the main basin of Nantucket Harbor (not all the way to the Sound). Local residence times for each sub-embayment are computed as:

$$T_{local} = \frac{V_{local}}{P} t_{cycle}$$

where T_{local} denotes the residence time for the local sub-embayment, V_{local} represents the volume of the sub-embayment at mean tide level, P equals the tidal prism (or volume entering the local sub-embayment through a single tidal cycle), and t_{cycle} the period of the tidal cycle (again, 0.52 days).

Residence times are provided as a first order evaluation of estuarine water quality. Lower residence times generally correspond to higher water quality; however, residence times may be misleading depending upon pollutant/nutrient loading rates and the overall quality of the receiving waters. As a qualitative guide, **system residence times** are applicable for systems where the water quality within the entire estuary is degraded and higher quality waters provide the only means of reducing the high nutrient levels. For the Nantucket Harbor system this approach is applicable, since it assumes the main system has relatively lower quality water relative to Nantucket Sound.

The rate of pollutant/nutrient loading and the quality of water outside the estuary both must be evaluated in conjunction with residence times to obtain a clear picture of water quality. It is impossible to evaluate an estuary's health based solely on flushing rates. Efficient tidal flushing (low residence time) is not an indication of high water quality if pollutants and nutrients are loaded into the estuary faster than the tidal circulation can flush the system. Neither are low residence times an indicator of high water quality if the water flushed into the estuary is of poor quality. Advanced understanding of water quality is obtained from the calibrated hydrodynamic model in the following section of this report (Section VI) by extending the model to include pollutant/nutrient dispersion. The water quality model provides an additional valuable tool to evaluate the complex mechanisms governing estuarine water quality in the Harbor system.

Since the calibrated RMA-2 model simulated accurate two-dimensional hydrodynamics in the system, model results were used to compute residence times. Residence times were computed for the entire estuary, as well the six sub-embayments within the system. In addition, **system** and **local residence times** were computed to indicate the range of conditions possible for the system.

Residence times were calculated as the volume of water (based on the mean volumes computed for the simulation period) in the entire system divided by the average volume of water exchanged with each sub-embayment over a flood tidal cycle (tidal prism). Units then were converted to days. The volume of the entire estuary was computed as cubic feet. Model divisions used to define the system sub-embayments include 1) the entire Nantucket Harbor system, 2) the Harbor from First Point, including Polpis Harbor and the Head of the Harbor, 3) the Head of the Harbor, 4) Polpis Harbor, 5) and The Creeks. These system divisions follow the model material type areas designated in Figure V-13. Sub-embayment mean volumes and tide prisms are presented in Table V-8.

Residence times were averaged for the tidal cycles comprising a representative 7 lunar day period (14 tide cycles), and are listed in Table V-9. The modeled time period used to compute the flushing rates started August 30, 2004, similar to the model calibration period, and included the transition from neap to spring tide conditions. The RMA-2 model calculated flow crossing specified grid lines for each sub-embayment to compute the tidal prism volume. Since the 7 lunar day period used to compute the flushing rates of the system represent average tidal conditions, the measurements provide the most appropriate method for determining mean flushing rates for the system sub-embayments.

The computed flushing rates for the Harbor system show that as a whole, the system flushes well. A flushing time of 1.6 days for the entire estuary shows that on average, water is resident in the system less than two days. All system sub-embayments have local flushing times that are equal to or less than 2 days. The Creeks has the shortest local flushing time, because this marsh has a small mean sub-embayment volume, relative to its tide prism.

The low local residence times in all areas of the Nantucket Harbor system show that they would likely have good water quality if the system water with which it exchanges also has good water quality. For example, the water quality of Polpis Harbor would likely be good as long as the water quality of the Harbor main basin was also good. Actual water quality would still also depend upon the total nutrient load to each embayment.

Table V-8. Embayment mean volumes and average tidal prism during simulation period.

Embayment	Mean Volume (ft^3)	Tide Prism Volume (ft^3)
Nantucket Harbor	1,984,232,000	646,811,000
Harbor from First Point	1,664,277,000	553,160,000
Head of the Harbor	752,681,000	274,938,000
Polpis Harbor	42,615,000	26,591,000
The Creeks	737,000	1,012,000

Table V-9. Computed System and Local residence times for embayments in the Nantucket Harbor system.

Embayment	System Residence Time (days)	Local Residence Time (days)
Nantucket Harbor	1.6	1.6
Harbor from First Point	1.9	1.6
Head of the Harbor	3.7	1.4
Polpis Harbor	38.6	0.8
The Creeks	1014.7	0.4

For the smaller sub-embayments of the Harbor system, computed system residence times are typically one or two orders of magnitude longer than their corresponding local residence time. System residence times provide a qualitative measure that helps to identify the relative sensitivity of different sub-embayments to nutrient loading.

Based on our knowledge of estuarine processes, we estimate that the combined errors associated with the method applied to compute residence times are within 10% to 15% of "true" residence times, for the Nantucket Harbor system. Possible errors in computed residence times can be linked to two sources: the bathymetry information and simplifications employed to calculate residence time. In this study, the most significant errors associated with the bathymetry data result from the process of interpolating the data to the finite element mesh, which was the basis for all the flushing volumes used in the analysis. In addition, limited topographic measurements were available in some of the smaller sub-embayments of the system.

Minor errors may be introduced in residence time calculations by simplifying assumptions. Flushing rate calculations assume that water exiting an estuary or sub-embayment does not return on the following tidal cycle. For regions where a strong littoral drift exists, this assumption is valid. However, water exiting a small sub-embayment on a relatively calm day may not completely mix with estuarine waters. In this case, the "strong littoral drift" assumption would lead to an under-prediction of residence time. Since littoral drift along the shoreline of Nantucket Sound typically is strong because of the effects of the local winds and tidal induced mixing within Nantucket Sound, the "strong littoral drift" assumption only will cause minor errors in residence time calculations.